

# Electron-Paramagnetic-Resonance Study of the Structure and Motions of $H_{AA}$ and $H_{A'A}$ Centers in $\text{Na}^+$ - and $\text{Li}^+$ -Doped $\text{KCl}^\dagger$

Dirk Schoemaker

Argonne National Laboratory, Argonne, Illinois 60439

(Received 3 December 1970)

Interstitial chlorine atoms in  $\text{KCl}$  can be stabilized by pairs of  $\text{Na}^+$  or  $\text{Li}^+$  impurity ions which are nearest neighbors (nn) and next nearest neighbors (nnn) of each other, forming what are called, respectively,  $H_{AA}$  and  $H_{A'A}$  centers. These centers have a higher thermal stability than the  $H_A$  (or  $V_i$ ) and  $H$  centers. Analysis of the electron-paramagnetic-resonance (EPR) spectra shows that the symmetries of  $H_{AA}(\text{Na}^+)$  and  $H_{AA}(\text{Li}^+)$  are the same and very similar to those of the  $H$  center: They each consist of a  $\langle 110 \rangle$ -oriented  $\text{Cl}_2^-$  molecule ion occupying a single negative-ion site and possessing weak molecular bonds with two neighboring substitutional  $\text{Cl}^-$  ions along  $\langle 110 \rangle$ . In contrast to the  $H$  center, the three molecular bonds of the  $\text{Cl}_2^-$  are bent in a  $\{001\}$  plane. It is concluded that the axis defined by the two adjoining nn impurity alkali ions is parallel to the  $\langle 110 \rangle$ -oriented  $\text{Cl}_2^-$  internuclear axis. This model does not allow any motion for the  $H_{AA}$  centers, and none is observed in the EPR spectra as the temperature is raised. The  $H_{A'A}$  centers consist of a  $\text{Cl}_2^-$  molecule ion, occupying a single negative-ion site associated with two  $\text{Na}^+$  or  $\text{Li}^+$  ions which are nnn of each other. However, the geometries of  $H_{A'A}(\text{Li}^+)$  and  $H_{A'A}(\text{Na}^+)$  are different. The  $H_{A'A}(\text{Li}^+)$  geometry is qualitatively similar to that of the  $H_A(\text{Li}^+)$  center: The  $\text{Cl}_2^-$  axis makes an  $18.5^\circ$  angle with  $\langle 001 \rangle$  in a  $\{110\}$  plane. The geometry of  $H_{A'A}(\text{Na}^+)$  is qualitatively similar to that of the  $H_A(\text{Na}^+)$  center: The  $\text{Cl}_2^-$  axis is tipped  $11.5^\circ$  away from  $\langle 110 \rangle$  in a  $\{001\}$  plane. Both centers therefore possess four equivalent orientations around a given  $\langle 001 \rangle$ . These directions lie in  $\{110\}$  planes for  $H_{A'A}(\text{Li}^+)$  and  $\{100\}$  planes for  $H_{A'A}(\text{Na}^+)$ . As the temperature is raised, the  $\text{Cl}_2^-$  is thermally activated among these four directions, and motionally averaged  $H_{A'A}(\text{Li}^+)$ - and  $H_{A'A}(\text{Na}^+)$ -center EPR spectra are observed corresponding to these two types of restricted pyramidal jumping motions.

## I. INTRODUCTION

Below 40 K, interstitial chlorine atoms ( $\text{Cl}_i^0$ ) produced by x or  $\gamma$  irradiation in pure  $\text{KCl}$  are stabilized as  $H$  centers,<sup>1,2</sup> i. e., essentially as  $\text{Cl}_2^-$  molecule ions each occupying one negative-ion site. In two recent papers<sup>3,4</sup> it was shown by a combined electron-paramagnetic-resonance (EPR) and optical-absorption investigation that mobile interstitial chlorine atoms produced by x or  $\gamma$  irradiation at 77 K can be trapped and stabilized as  $H$ -type centers by  $\text{Na}^+$  or  $\text{Li}^+$  impurity alkali ions in  $\text{KCl}$ . Optical investigations on  $\text{Na}^+$ - and  $\text{Li}^+$ -doped  $\text{KBr}$  have also been performed recently.<sup>5,6</sup> For historical reasons these centers were called  $V_1(\text{Na}^+)$  and  $V_1(\text{Li}^+)$  centers. However, it was suggested<sup>4</sup> that  $H_A(\text{Na}^+)$  and  $H_A(\text{Li}^+)$  would be a more generic notation, and this notation will be adopted in this paper. In the course of these  $H_A$ -center studies it was found that at higher  $\text{Na}^+$ - or  $\text{Li}^+$ -doping concentrations two other  $H$ -type centers could be produced in  $\text{KCl}$ , and the EPR study of these centers is the subject of this paper. As will be shown, these two centers are created when interstitial chlorine atoms are trapped and stabilized by pairs of  $\text{Na}^+$  or  $\text{Li}^+$  impurity ions which are, respectively, nearest neighbors (nn) and next nearest neighbors (nnn) of each other. These centers, in an obvious extension of

the foregoing notation, will be called, respectively,  $H_{AA}$  and  $H_{A'A}$  centers. Thus in strongly doped  $\text{KCl}:\text{Na}^+$ ,  $H_{AA}(\text{Na}^+)$  and  $H_{A'A}(\text{Na}^+)$  centers are observed, and similarly  $H_{AA}(\text{Li}^+)$  and  $H_{A'A}(\text{Li}^+)$  in strongly doped  $\text{KCl}:\text{Li}^+$ . The knowledge of the structure and properties of these centers may prove to be useful in theoretical treatments of interstitial stabilization in alkali halides.<sup>7</sup> However, our immediate interest in the study of these centers stems from the fact that the  $H_{A'A}$  centers, in particular, exhibit restricted motions the study of which has contributed to a better understanding of the motions exhibited by the  $H_A(\text{Na}^+)$ <sup>3</sup> and  $H_A(\text{Li}^+)$  centers. Apart from their production (Sec. III), the properties of the  $H_{AA}$  and  $H_{A'A}$  centers are sufficiently different from each other ( $H_{AA}$ , e. g., shows no motional effects) so that they will be treated separately;  $H_{AA}$  in the first part (Sec. IV) and  $H_{A'A}$  in the second part (Secs. V and VI) of this paper. In order to eliminate any possible ambiguity, it is stressed here that the terms nn and nnn, as used in this paper, always and exclusively refer to the relative position of the two impurity alkali ions ( $\text{Na}^+$  or  $\text{Li}^+$ ) with respect to each other, and not with respect to the interstitial.

## II. EXPERIMENTAL

The crystals used in these experiments were

grown in air by the Kyropoulos method using very pure KCl (very low  $\text{Br}^-$  and divalent alkaline-earth ion concentrations) starting material. Several  $\text{KCl}:\text{Na}^+$  crystals were grown from KCl melts to which between 1.0 and 4.0 wt% of NaCl was added. The very strongly doped (4.0 wt%)  $\text{KCl}:\text{Na}^+$  specimens often deteriorate after several weeks. The specimens recrystallize randomly at various spots, mainly around edge and corner cracks, and become cloudy. The less strongly doped crystals (1.0–2.0 wt%) do not show this behavior and they were generally used. The  $\text{KCl}:\text{Li}^+$  crystals were grown from melts with up to 1.5 wt% of LiCl. Though these crystals do not recrystallize or cloud up after a few weeks, there is evidence from the EPR spectra that the  $\text{Li}^+$  ions tend to aggregate. This has been observed before.<sup>8</sup> It was found that the  $\text{Li}^+$  ions can be dispersed again, probably to random distribution, by heating the  $\text{KCl}:\text{Li}^+$  specimens to  $\sim +500^\circ\text{C}$  and rapid cooling to room temperature. Therefore the  $\text{KCl}:\text{Li}^+$  specimens were always routinely subjected to this treatment before  $x$  or  $\gamma$  irradiation.

The color centers were produced by  $x$  or  $\gamma$  irradiation at 77 K. The  $\gamma$  rays were supplied by an 18 000-Ci  $^{60}\text{Co}$  source and the  $x$  rays by a Machlett tube operating at 60 kV and 40 mA. The irradiation time in both cases was usually at least 4 h or longer. Details on the EPR measurements have been given before.<sup>3</sup>

### III. PRODUCTION OF $H_{AA}$ and $H_{A'A}$ CENTERS

Both the  $H_{AA}$  and  $H_{A'A}$  centers in KCl are interstitial centers formed by trapping an interstitial chlorine atom by pairs of  $\text{Na}^+$  or  $\text{Li}^+$  ions which are, respectively, nn and nnn of each other. The probability of having such nn or nnn pairs is negligibly small for small doping concentrations ( $\sim 0.1$  wt%), and in these crystals the  $H_{AA}$  and  $H_{A'A}$  centers are not observed experimentally. However, the probability of having nn and nnn pairs increases rapidly with the impurity concentration (quadratically, if the distribution is purely random), and indeed, reasonable concentrations of  $H_{AA}$  and  $H_{A'A}$  are obtained experimentally when the doping levels of NaCl and LiCl in the KCl melt are  $\geq 1.0$  wt%.

The production of  $H_{AA}$  and  $H_{A'A}$  is straightforward and we shall first discuss the  $\text{KCl}:\text{Na}^+$  system. The crystal is irradiated with  $x$  or  $\gamma$  rays at 77 K. This irradiation produces as primary defects electrons, holes, interstitial halogen atoms, interstitial halogen ions, and negative-ion vacancies ( $\alpha$  centers). The electrons are mainly trapped by the negative-ion vacancies and form  $F$  centers. The holes become mostly self-trapped at 77 K and form  $\text{Cl}_2^-$  centers ( $V_K$  centers).<sup>9,10</sup> However, since the concentration of the  $\text{Na}^+$  impurity is quite high, a small fraction of the holes is

trapped next to  $\text{Na}^+$  ions, forming  $V_{KA}(\text{Na}^+)$  centers, i. e.,  $V_K$  centers associated with a  $\text{Na}^+$  impurity.<sup>11,12</sup> The interstitial chlorine atoms, on the other hand, are very mobile at 77 K (the  $H$  center is unstable above  $\sim 40$  K), and most of them are trapped by the substitutional  $\text{Na}^+$  impurities, forming  $H_A(\text{Na}^+)$  [or  $V_1(\text{Na}^+)$ ] centers.<sup>3,13</sup> However, since we are working with high  $\text{Na}^+$  concentrations, the nn and nnn pairs of  $\text{Na}^+$  also trap interstitial Cl atoms and, consequently,  $H_{AA}(\text{Na}^+)$  and  $H_{A'A}(\text{Na}^+)$  centers are already visible in the EPR spectra. The EPR spectra of  $H_{AA}(\text{Na}^+)$  and  $H_{A'A}(\text{Na}^+)$  can be isolated and their intensities enhanced. First, the  $\text{Cl}_2^-$  centers [ $V_K$  and  $V_{KA}(\text{Na}^+)$ ], which possess a positive charge with respect to the lattice, are preferentially bleached out. This is accomplished through optical excitation of  $F$  centers (a few minutes with an HBO-500 lamp + No. 3480 Corning glass filter), and the electrons thus released recombine preferentially with the  $\text{Cl}_2^-$  centers.<sup>14</sup> The concentrations of  $H_A(\text{Na}^+)$ ,  $H_{AA}(\text{Na}^+)$ , and  $H_{A'A}(\text{Na}^+)$  are hardly affected by this treatment. This indicates that  $H_{AA}(\text{Na}^+)$  and  $H_{A'A}(\text{Na}^+)$  are very likely also neutral centers just as  $H_A(\text{Na}^+)$ , further indicating their interstitial character. The crystal is then warmed up. The  $H_A(\text{Na}^+)$  center decays thermally at 110 K because the interstitial chlorine atom breaks away from around the  $\text{Na}^+$ . A number of these interstitials recombine with  $F$  centers to reestablish the perfect lattice at these spots. Other interstitial Cl atoms combine with  $\alpha$  centers and as a result  $V_K$  centers are formed. Finally, a number of interstitials are retrapped by the nn and nnn pairs of  $\text{Na}^+$  ions, increasing the concentration of  $H_{AA}(\text{Na}^+)$  and  $H_{A'A}(\text{Na}^+)$ . These EPR observations (except those in connection with the  $F$  center) are illustrated in Fig. 1 which gives the pulse-anneal results of an irradiated  $\text{KCl}:\text{Na}^+$  crystal. In these experiments the crystal was warmed to a certain temperature, held there for 2 min, and then cooled to 77 K, where the changes in the EPR spectra were measured. This procedure was then repeated with temperatures which were successively  $10^\circ$  higher.<sup>15</sup> The relative intensities of the centers in Fig. 1 are purely qualitative, and depend, e. g., on the length of the  $\gamma$  irradiation and the  $\text{Na}^+$  concentration. At this point in the pulse anneal (i. e., at 110 K) one can again eliminate optically the small amount of  $V_K$  centers since these interfere with the EPR spectra of  $H_{AA}(\text{Na}^+)$  and  $H_{A'A}(\text{Na}^+)$ . Continuing the pulse anneal one observes that the  $H_{AA}(\text{Na}^+)$  centers decay at 140 K [increasing  $H_{A'A}(\text{Na}^+)$  somewhat] and that the  $H_{A'A}(\text{Na}^+)$  centers decay at 158 K. Both decays result in the formation of  $V_K$  centers. If these  $V_K$  centers are not bleached out optically, but are allowed to decay thermally, some of the holes are retrapped by the  $\text{Na}^+$  ions and one observes the formation of  $V_{KA}(\text{Na}^+)$

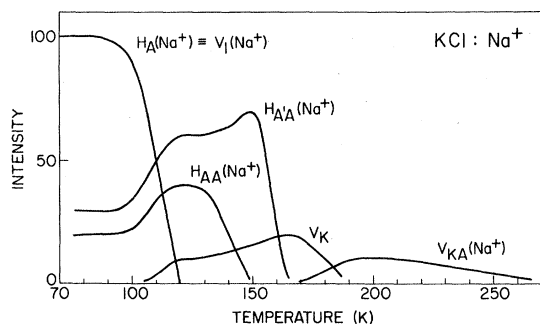
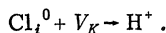


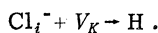
FIG. 1. Pulse-anneal results on a strongly doped KCl:Na<sup>+</sup> crystal performed after several hours of  $\gamma$  irradiation at 77 K and a subsequent optical bleach of the Cl<sub>2</sub><sup>-</sup> centers. The relative intensities of the various centers are arbitrary.

centers. These  $V_{KA}(\text{Na}^+)$  centers decay above 220 K.

The previous pulse anneal was started after the  $V_K$  centers had been bleached out optically. However, if such an optical bleach is not done, the pulse-anneal results look somewhat different. It is observed that as  $H_A(\text{Na}^+)$  decays, a large fraction of the  $V_K$  centers decays too at the same rate. This effect is also strong, if not stronger, in the lightly doped KCl:Na<sup>+</sup> crystals. Though this has not yet been studied further it may be of some interest to offer a speculation here. If one limits oneself to the simplest explanation of this observation—namely, a direct recombination of a mobile Cl<sub>i</sub><sup>0</sup> with a  $V_K$  center—one is led to the existence of a neutral Cl<sub>2</sub> molecule (unobservable by EPR) occupying a single negative-ion site, and one could call this an  $H^+$  center. Such a reaction could be written as



This reaction would be very analogous to the following one which occurs at about 32 K where the interstitial chlorine ion Cl<sub>i</sub><sup>-</sup> apparently becomes mobile<sup>16</sup>:



The production of  $H_{AA}(\text{Li}^+)$  and  $H_{A'A}(\text{Li}^+)$  in strongly doped KCl:Li<sup>+</sup> is very similar to the foregoing, the main difference being that the  $H_A(\text{Li}^+)$ ,  $H_{AA}(\text{Li}^+)$ , and  $H_{A'A}(\text{Li}^+)$  have a substantially higher thermal stability than the corresponding Na<sup>+</sup> stabilized centers. Figure 2 presents the results of a pulse-annealing experiment on a KCl:Li<sup>+</sup> crystal which had been  $\gamma$  irradiated at 77 K, and in which the Cl<sub>2</sub><sup>-</sup> centers had been bleached out optically. The  $H_A(\text{Li}^+)$  center decays at 230 K enhancing the  $H_{AA}(\text{Li}^+)$  and  $H_{A'A}(\text{Li}^+)$  concentrations. The  $V_K$  centers formed when some of the Cl<sub>i</sub><sup>0</sup> combine with  $\alpha$  centers, are not stable at this temperature. These mobile  $V_K$  centers are, however, quickly stabilized next to the Li<sup>+</sup> ions, and  $V_{KA}(\text{Li}^+)$  centers<sup>11</sup> are

formed. These  $V_{KA}(\text{Li}^+)$  centers, which are also positively charged with respect to the lattice, can again be bleached out preferentially by optical excitation of the  $F$  centers. As was the case for  $H_{AA}(\text{Na}^+)$  and  $H_{A'A}(\text{Na}^+)$ , it is also found that  $H_{A'A}(\text{Li}^+)$  has a slightly higher thermal stability than  $H_{AA}(\text{Li}^+)$ .  $H_{AA}(\text{Li}^+)$  and  $H_{A'A}(\text{Li}^+)$  decay at 265 and 283 K, respectively, enhancing the  $V_{KA}(\text{Li}^+)$  concentration. The  $V_{KA}(\text{Li}^+)$  center decays at 310 K.

Finally, we would like to underline the importance of growing the crystals from very pure KCl starting material. If the KCl material contains a sizeable amount of Br<sup>-</sup> ions, as is often the case, one produces  $H_A(\text{Na}^+)$ -type BrCl<sub>2</sub><sup>-</sup> centers or  $H_A(\text{Li}^+)$ -type BrCl<sup>-</sup> centers<sup>4,17</sup> whose EPR spectra interfere with the weak  $H_{AA}$  and  $H_{A'A}$  EPR spectra. Divalent cations also give rise to interfering EPR spectra.<sup>18</sup>

#### IV. $H_{AA}$ CENTERS

##### A. EPR Spectra

The  $H_{AA}(\text{Na}^+)$  EPR spectra in KCl:Na<sup>+</sup> recorded at 115 K for three special orientations of the magnetic field  $\vec{H}$  are shown in Fig. 3. As described in more detail in Sec. III these spectra were obtained after (a) several hours of  $\gamma$  irradiation at 77 K; (b) elimination of the  $V_K$ -type Cl<sub>2</sub><sup>-</sup> centers by optically exciting  $F$  centers at 77 K; (c) a warm up to 120 K for a few minutes to eliminate the  $H_A(\text{Na}^+)$  centers and a concurrent or subsequent bleach into the  $F$  band to eliminate the newly created  $V_K$  centers. After this treatment the EPR spectra of both  $H_{AA}(\text{Na}^+)$  and  $H_{A'A}(\text{Na}^+)$  are present. However, the presence of  $H_{A'A}(\text{Na}^+)$  does not interfere too much with the analysis of  $H_{AA}(\text{Na}^+)$ . The  $H_{AA}(\text{Na}^+)$  EPR lines are quite narrow ( $\sim 2$  G) and well resolved, and require a low peak-to-peak field modulation for good resolution. Furthermore, the lines are quite saturable, and the spectra must be recorded at low powers ( $\sim 20$  dB at 115 K). The  $H_{A'A}(\text{Na}^+)$  EPR lines, on the other hand, are quite broad ( $\sim 10$  G), requiring for an optimum signal-to-noise ratio the use of larger field modulation am-

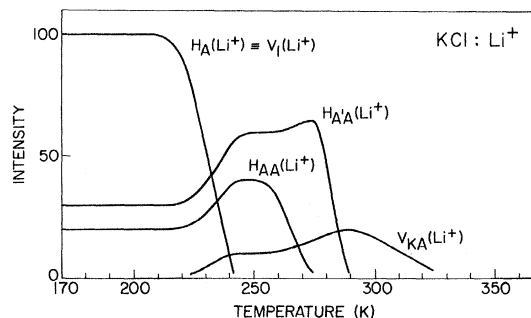


FIG. 2. Same as Fig. 1 but for a strongly doped KCl:Li<sup>+</sup> crystal.

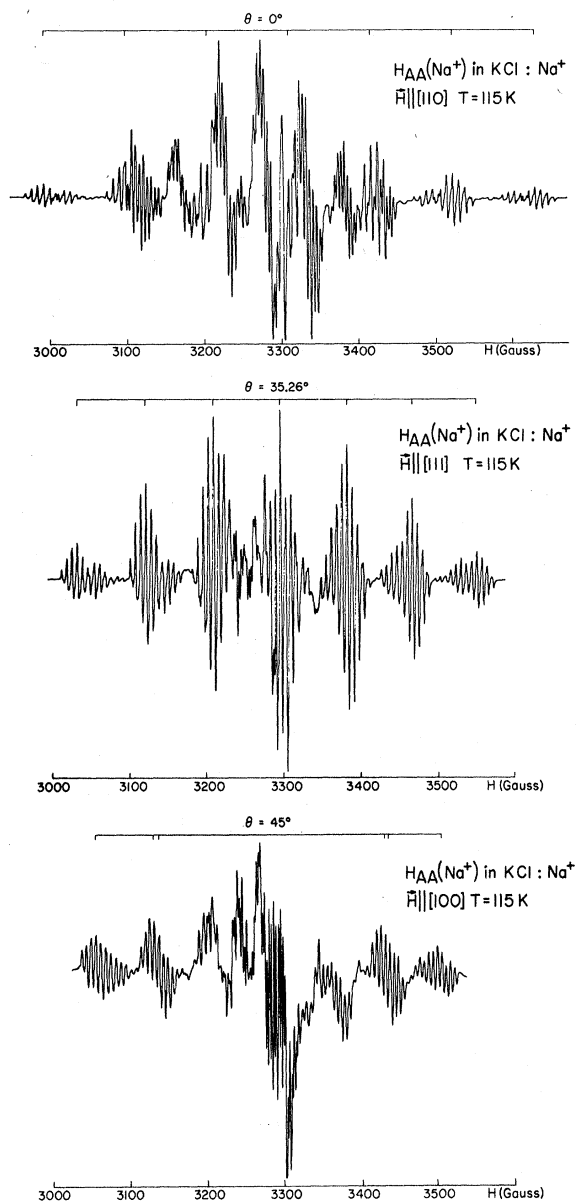


FIG. 3. The  $H_{AA}(\text{Na}^+)$  EPR spectra in  $\text{KCl}:\text{Na}^+$  for three orientations of the magnetic field  $\vec{H}$  recorded at 115 K. Microwave frequency  $\nu = 9.273$  GHz. The broader underlying lines originate from the  $H_{A'A}(\text{Na}^+)$  center. The first derivative of the absorption is presented.

plitudes. Furthermore, the lines do not saturate even at the highest available microwave powers ( $\sim 125$  mW). Thus the circumstances under which the  $H_{AA}(\text{Na}^+)$  signals must be recorded for optimum resolution suppress to a large extent the  $H_{A'A}(\text{Na}^+)$  EPR signals. The amount of interference can be judged from Fig. 3: Only the stronger central  $H_{A'A}(\text{Na}^+)$  lines are visible under the narrow  $H_{AA}(\text{Na}^+)$  lines. It should be noted that there is a definite quantitative difference in relaxation be-

havior between  $H_{AA}(\text{Na}^+)$  and  $H_{AA}(\text{Li}^+)$ . Such a difference, but an even more pronounced one, has also been noted between the  $H_A(\text{Na}^+)$  and  $H_A(\text{Li}^+)$  centers.<sup>4</sup> The  $H_{AA}(\text{Na}^+)$  EPR signals are much more saturable with microwave power than the  $H_{AA}(\text{Li}^+)$  signals. In fact the spin-lattice relaxation time of  $H_{AA}(\text{Na}^+)$  is still quite long at 77 K. It increases as the temperature is raised, and it is observed that for the same power level ( $-20$  dB) the  $H_{AA}(\text{Na}^+)$  signal is about 50% stronger at 115 K than at 77 K. No similar effect is observed for  $H_{AA}(\text{Li}^+)$  as the temperature is raised.

Comparison of the spectra in Fig. 3 with the published EPR spectra of the  $H$  center,<sup>1,3</sup> makes it immediately clear that one is dealing with a center which in symmetry and appearance is very similar to the  $H$  center. In particular, the  $H_{AA}(\text{Na}^+)$  center is oriented exactly along  $\langle 110 \rangle$ . References 1 and 3 give a detailed analysis of the  $H$ -center EPR spectra. The characteristic seven groups of lines, with intensity ratios 1:2:3:4:3:2:1, are easily observable in the  $\theta = 0^\circ$  ( $\vec{H} \parallel \langle 110 \rangle$ ) and  $\theta = 35.26^\circ$  ( $\vec{H} \parallel \langle 111 \rangle$ ) spectra, indicating hf interaction with two equivalent (for these two orientations at least) central chlorine nuclei (1 and 2 in Fig. 4) whose isotopes ( $^{35}\text{Cl}$  and  $^{37}\text{Cl}$ ) all have nuclear spin  $\frac{3}{2}$ . Furthermore, for  $\theta = 0^\circ$  and  $\theta = 35.26^\circ$  each line group consists also of seven lines with intensity ratios 1:2:3:4:3:2:1, indicating a further weaker super hyperfine (shf) interaction with two other Cl nuclei (3 and 4 in Fig. 4). However, the difference between the  $H$  and  $H_{AA}(\text{Na}^+)$  EPR spectra is obvious in the  $\theta = 45^\circ$  ( $\vec{H} \parallel \langle 100 \rangle$ ) spectra, where the 1:2:3:4:3:2:1 ratios are *not* observed, either for the main seven groups of lines, or for the seven-line structure inside each group. This means that for  $H_{AA}(\text{Na}^+)$  the central chlorine nuclei (1, 2), and also nuclei (3, 4), are not equivalent for all orientations of the magnetic field. One concludes, and this is supported by a careful angular-variation study, that not only the strong molecular bond 1-2, but also the weaker molecular bonds 3-1 and 2-4 are bent in a  $\{100\}$  plane (the latter two by exactly the same amount because of symmetry considerations). The bending of the molecular bond makes nuclei 1 and 2, and similarly nuclei 3 and 4, equivalent only when the magnetic field is either in the plane perpendicular to the 1-2 internuclear axis (which is parallel to the 3-4 internuclear axis), or in a plane perpendicular to the plane of the bending and parallel to the 1-2 (or 3-4) internuclear axis. The presence of bending is even more obvious in the EPR spectra of  $H_{AA}(\text{Li}^+)$ . The  $\theta = 0^\circ$  and  $\theta = 35.26^\circ$   $H_{AA}(\text{Li}^+)$  EPR spectra are well defined and qualitatively indistinguishable to the ones in Fig. 3 (or, for that matter, to the corresponding  $H$ -center EPR spectra). However, for  $H_{AA}(\text{Li}^+)$  the bendings of the three molecular bonds are so large that the  $\theta = 45^\circ$  spectrum

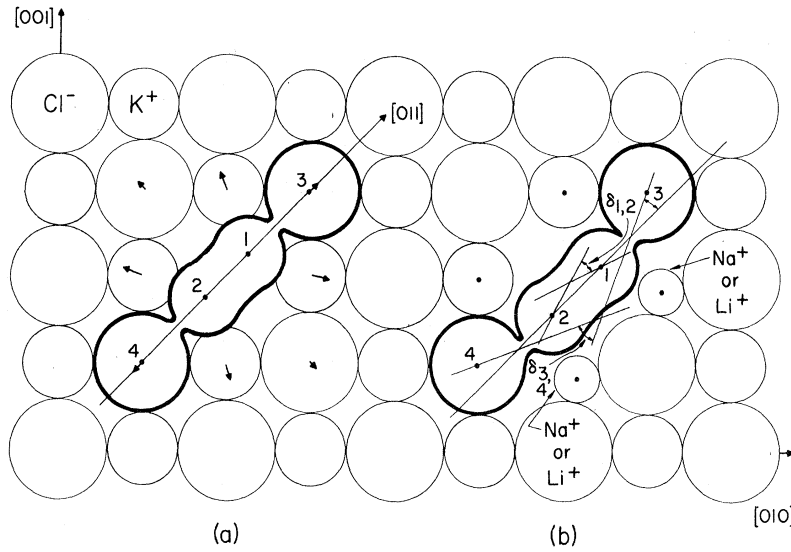


FIG. 4. Schematic representation of the models of (a) the  $H$  center and (b) the  $H_{AA}$  centers in KCl. Both  $H_{AA}(\text{Na}^+)$  and  $H_{AA}(\text{Li}^+)$  have the same geometry. Displacement of the lattice around the  $H$  center (from Ref. 21) is indicated qualitatively.

( $\vec{H} \parallel \langle 100 \rangle$ ) is completely garbled up and unrecognizable.

The  $H_{AA}$  EPR spectra were matched to the following spin Hamiltonian:

$$\frac{\mathcal{H}}{g_0 \mu_B} = \frac{1}{g_0} \vec{H} \cdot \vec{g} \cdot \vec{S} + \sum_{i=1}^4 \vec{S} \cdot \vec{A}_i \cdot \vec{I}_i + \sum_{i=1}^2 P I_{zi}^2. \quad (1)$$

The magnitudes of  $\vec{A}_1$  and  $\vec{A}_2$  are the same (i.e.,  $\det \vec{A}_1 = \det \vec{A}_2$ ), but because of the bending, their symmetry axes do not coincide. The direction of the symmetry axes is given in Fig. 4: They are the directions defining the bending angle  $\delta_{1,2}$ . Similarly,  $\det \vec{A}_3 = \det \vec{A}_4$ , and their symmetry axes are given in Fig. 4 by the lines that define  $\delta_{3,4}$ . The high symmetry of the  $H_{AA}$  center dictates that the  $\vec{g}$ -tensor symmetry axis lies along the internuclear axis 1-2 (or 3-4), i.e., exactly along  $\langle 110 \rangle$  which is defined as the  $z$  direction. Not enough lines could be measured with sufficient precision to de-

termine the quadrupole parameter  $P$ , but the results for the  $H$  center<sup>3</sup> [ $P = (-5.7 \pm 2)$  G] and the  $V_K$  center<sup>19</sup> [ $P = (-4.8 \pm 0.5)$  G] indicate that  $P = (-5 \pm 2)$  G should be a reasonable value. Neglecting the small effect caused by the fact that the  $\vec{g}$  and  $\vec{A}_i$  axes do not coincide, the angular variation of the first-order hf separations  $K_i$  (in axial approximation) and the  $g$  factor are given by

$$K_i^2(\theta) g^2(\theta) = A_{\parallel, i}^2 g_{\parallel}^2 \cos^2 \theta + A_{\perp, i}^2 g_{\perp}^2 \sin^2 \theta$$

$$g^2(\theta, \varphi) = g_{\parallel}^2 \cos^2 \theta + g_x^2 \sin^2 \theta \cos^2 \varphi + g_y^2 \sin^2 \theta \sin^2 \varphi. \quad (2)$$

For each  $K_i$ , the  $\theta$  is measured from the  $\vec{A}_i$  symmetry axis, and for the  $g$  factor,  $\theta$  is measured from the  $\vec{g}$ -tensor symmetry axis.

The bending angles of the molecular bonds 1-2, 3-1, and 2-4 have been determined through an angular-variation study of the EPR spectra in a

TABLE I. Spin-Hamiltonian parameters of the  $H$ ,  $H_{AA}(\text{Na}^+)$ , and  $H_{AA}(\text{Li}^+)$  centers at, respectively, 25, 115, and 77 K. The hf parameters and the linewidths  $\Delta H$  (between extrema of the first derivative) are expressed in G. The internuclear axes of these centers are exactly along  $\langle 110 \rangle$ , and  $\delta_{1,2}$  and  $\delta_{3,4}$  are the bending angles of molecular bonds (see Fig. 4).

Center	$g_z$ [110]	$g_x$ [001]	$g_y$ [110]	$A_{\parallel 1,2}$	$A_{\perp 1,2}$	$A_{\parallel 3,4}$	$A_{\perp 3,4}$	$P_{1,2}$	$\delta_{1,2}$ (deg)	$\delta_{3,4}$ (deg)	$\Delta H$	$T_{\text{decay}}$ (K)
$H$	2.0018 $\pm 0.0002$	2.0221 $\pm 0.0005$	2.0227 $\pm 0.0005$	108.6 <sup>a</sup> $\pm 0.1$	16.0 $\pm 1.5$	7.4 $\pm 0.1$	2.7 $\pm 0.1$	-5.7 $\pm 2$	0	0	1.2 $\pm 0.1$	42
$H_{AA}(\text{Na}^+)$	2.0018 $\pm 0.0002$	2.0235 $\pm 0.0005$	2.0261 $\pm 0.0005$	106.2 <sup>b</sup> $\pm 0.1$	12.5 $\pm 1.5$	7.9 $\pm 0.1$	3.6 $\pm 0.5$	...	3.2 $\pm 0.5$	6 $\pm 2$	1.9 $\pm 0.1$	140
$H_{AA}(\text{Li}^+)$	2.0019 $\pm 0.0002$	2.0273 $\pm 0.0005$	2.034 $\pm 0.001$	104.1 <sup>c</sup> $\pm 0.2$	11.0 $\pm 2$	7.1 $\pm 0.2$	2.4 $\pm 1$	...	10 $\pm 2$	15 $\pm 5$	2.3 $\pm 0.1$	265

<sup>a</sup>At 4.2 K,  $A_{\parallel 1,2} = 109.1$  G.

<sup>b</sup>At 77 K,  $A_{\parallel 1,2} = 106.8$  G.

<sup>c</sup>At 115 K,  $A_{\parallel 1,2} = 103.8$  G.

{100} plane, starting from a  $\langle 110 \rangle$  direction. For  $H_{AA}(\text{Li}^+)$  at  $\theta = 20^\circ$ , it is observed that the degenerate lines of the shf splitting from nuclei 3 and 4 are split by  $\Delta K_{3,4} \approx 0.5$  G ( $K_{3,4} = 6.5$  G). At  $\theta = 20^\circ$  the degenerate lines of the primary hf splitting arising from nuclei 1 and 2 are split by  $\Delta K_{1,2} \approx 6.5$  G ( $K_{1,2} = 97.2$  G). The bending angles are then obtained by using

$$\delta = \Delta\theta = \frac{K_i \Delta K_i}{(A_{ii}^2 - A_{Li}^2) \sin\theta \cos\theta}, \quad (3)$$

which is obtained by differentiating the expression for  $K_i$  as given in (2), ignoring the small  $g$  anisotropy. The results for the  $H_{AA}(\text{Na}^+)$  and  $H_{AA}(\text{Li}^+)$  centers are given in Table I, together with the  $H$ -center parameters. This table shows that (a) the primary hf interaction decreases and (b) the perpendicular  $g$  shift  $\Delta g_\perp = g_\perp - g_0$  [in which  $g_\perp = \frac{1}{2} \times (g_x + g_y)$ ] increases, if one goes from  $H$  to  $H_{AA}(\text{Na}^+)$  to  $H_{AA}(\text{Li}^+)$ . These observations are consistent<sup>4</sup> with the assumption that there is a very small increase in the internuclear distance of the central nuclei 1 and 2 in going from  $H$  to  $H_{AA}(\text{Na}^+)$  to  $H_{AA}(\text{Li}^+)$ . The behavior of  $\Delta g_\perp$  furthermore indicates<sup>4</sup> that the optical-absorption bands of  $H_{AA}(\text{Na}^+)$  and  $H_{AA}(\text{Li}^+)$  will occur at progressively lower energies than those of the  $H$  center. The latter are positioned at 338 and 522 nm.<sup>2</sup> Optical-absorption measurements on the  $H_{AA}(\text{Na}^+)$  and  $H_{AA}(\text{Li}^+)$  centers were not attempted because the  $H_{A'A}(\text{Na}^+)$  and  $H_{A'A}(\text{Li}^+)$  centers, whose optical-absorption bands are expected to overlap strongly with the  $H_{AA}$  centers, are always present.

#### B. Model for $H_{AA}$ Centers

A summary of the observations which lead to the model of the  $H_{AA}$  center, as depicted in Fig. 4, is as follows: (a)  $H_{AA}$  is observable only in strongly doped KCl:Na<sup>+</sup> or KCl:Li<sup>+</sup> crystals, suggesting that more than one, i.e., very likely two, impurity alkali ions are involved. (b) When  $H_A$  decays thermally,  $H_{AA}$  is formed, i.e.,  $H_{AA}$  is likely to be an interstitial center produced by retrapping of the mobile interstitial Cl atom originating from a thermally decaying  $H_A$ . (c)  $H_{AA}$  is very likely a neutral center since it is not affected much when  $F$  centers are optically excited. (d)  $H_{AA}$  is oriented exactly along  $\langle 110 \rangle$ . (e)  $H_{AA}$  comprises a  $\text{Cl}_2^-$  molecule ion whose nuclei 1 and 2 are equivalent for certain orientations of the magnetic field. (f)  $H_{AA}$  shows a small shf structure originating from two other Cl nuclei, 3 and 4, which are also equivalent for the same orientations of  $\vec{H}$ . (g) The molecular bonds 1-2, 3-1, and 2-4 are bent in the same {100} plane. The proposed  $H_{AA}$ -center model shown in Fig. 4 explains all these observations, as one can easily verify. In fact it appears to be the only possible

model involving two impurity alkali ions; e.g., if the  $\text{Na}^+ - \text{Na}^+$  axis of the two nn Na<sup>+</sup> ions were perpendicular to the 1-2 molecular axis, one would probably still have a  $\langle 110 \rangle$ -oriented center but the four Cl nuclei would be definitely inequivalent.<sup>20</sup> Also, it would not be possible to explain the observed bendings. If the two Na<sup>+</sup> ions were nn's, then, either they would not produce a  $\langle 110 \rangle$ -oriented center, or if they did (e.g., if the  $\text{Na}^+ - \text{Na}^+$  axis along [001] were perpendicular to the 1-2 molecular axis along [110]), one could not explain the bendings of the molecular bonds in the (001) plane. Furthermore, the  $H_{A'A}$ -center EPR spectra, to be discussed in the second half of this paper, are readily explained with models involving two Na<sup>+</sup> or Li<sup>+</sup> ions which are nn of each other.

It should be pointed out that the EPR analysis does not yield the sense of the bending of the three molecular bonds. The choice made in Fig. 4 seems to be a reasonable one: The weaker bonds, 1-3 and 4-2, are likely bent towards the Na<sup>+</sup> or Li<sup>+</sup> ions, while the strong 1-2 bond is believed to be bent towards the center of the negative-ion vacancy which the  $\text{Cl}_2^-$  occupies. This is probably true because the  $\text{Cl}_2^-$  is very likely displaced away from the center of this vacancy in the direction of the two nn alkali-ion impurities.

A recent determination of the strain field around the  $H$  center in KBr<sup>21</sup> (which has the same symmetry and properties as the  $H$  center in KCl) also makes the  $H_{AA}$  model in Fig. 4(a) a plausible one. It was found that the four K<sup>+</sup> ions surrounding the diatomic molecule ion in the (001) plane are pushed out substantially (about 11% of the anion-cation distance in KBr). Clearly, the strain field around the  $H$  center will be progressively reduced if two K<sup>+</sup> ions on one side of the  $\text{Cl}_2^-$  molecular axis are replaced by the smaller Na<sup>+</sup> or Li<sup>+</sup> ions. The  $\text{Cl}_2^-$  will have a little more room and can presumably relax to a slightly larger 1-2 internuclear distance. The interpretation of the EPR results at the end of Sec. IV A is consistent with this reasoning.

Closer inspection of the proposed  $H_{AA}$  center model in Fig. 4 shows that it has no possibility for thermal reorientation into an equivalent orientation, i.e., the  $H_{AA}$  center is a rigid center. The  $H_{AA}(\text{Na}^+)$  and  $H_{AA}(\text{Li}^+)$  EPR lines show indeed no trace of lifetime broadening of any kind (very rapid rotational or jumping motion of the center, or fast spin-lattice relaxation), even at the decay temperatures of these centers. This is another observation in favor of the proposed  $H_{AA}$ -center model.

It is well known that the Na<sup>+</sup> and Li<sup>+</sup> impurities behave differently in KCl: The very small Li<sup>+</sup> ion is displaced off-center along a  $\langle 111 \rangle$  direction,<sup>8</sup> while the Na<sup>+</sup> ion remains on its lattice site. It is believed that this actual (or incipient in the case of<sup>4</sup> KBr:Li<sup>+</sup>) off-center behavior of the Li<sup>+</sup> ion is

basically responsible for the difference in symmetry that has been observed between the  $H_A(\text{Li}^+)$  and  $H_{AA}(\text{Na}^+)$  centers in KCl.<sup>4</sup> However, apart from the fact that the bending angles  $\delta_{1,2}$  and  $\delta_{3,4}$  are bigger for  $H_{AA}(\text{Li}^+)$  than for  $H_{AA}(\text{Na}^+)$  (which seems reasonable in view of the smaller size of the  $\text{Li}^+$  ion), the symmetries of  $H_{AA}(\text{Li}^+)$  and  $H_{AA}(\text{Na}^+)$  appear to be identical. No off-center effects, peculiar to the  $\text{Li}^+$  ion, have been detected. One could, e.g., expect that the bending of the three molecular bonds would be outside the  $\{001\}$  plane because the two  $\text{Li}^+$  ions could be displaced a bit outside the  $(001)$  plane in Fig. 3 (either above or below). However, a measurable tilting of the bending plane with respect to  $\{001\}$  would destroy the exact 1:2:3:4:3:2:1 intensity distribution of the hf and shf structure observed in the  $\theta = 35.26^\circ$  spectrum ( $\vec{H} \parallel \langle 111 \rangle$ ), because the degenerate lines would tend to split. No such effect has been observed for  $H_{AA}(\text{Li}^+)$ . Hence, within the accuracy of the observations, the bending plane coincides with a  $\{001\}$  plane.

To end this section we should mention that we have observed the  $H_{AA}(\text{Na}^+)$  center in strongly doped  $\text{KBr}:\text{Na}^+$ . Furthermore, interstitial bromine and iodine atoms, trapped by two nn  $\text{Na}^+$  in strongly doped  $\text{KCl}:\text{Na}^+$ ,  $\text{Br}^-$  and  $\text{KCl}:\text{Na}^+$ ,  $\text{I}^-$  crystals, have also been observed. The latter centers manifest themselves as linear and symmetric (i. e., of the type  $\text{XYX}^{--}$ )  $\langle 110 \rangle$ -oriented  $\text{BrCl}_2^{--}$  and  $\text{ICl}_2^{--}$  centers in which the Br and I occupy the interstitial position between the two substitutional and equivalent  $\text{Cl}^-$  ions and between the two substantial  $\text{Na}^+$  ions. The  $\text{Na}^+ - \text{Na}^+$  axis is therefore perpendicular to the  $\text{BrCl}_2^{--}$  internuclear axis. The latter two centers are different from the  $H_A$ -type  $\text{XYX}^{--}$  centers mentioned before.<sup>4,17</sup>

#### V. $H_{A'A}(\text{Li}^+)$ CENTER

In contrast to the  $H_{AA}(\text{Na}^+)$  and  $H_{AA}(\text{Li}^+)$  centers, there is a definite difference in symmetry between  $H_{A'A}(\text{Li}^+)$  and  $H_{A'A}(\text{Na}^+)$ . In fact, as we shall see, the symmetry of  $H_{A'A}(\text{Li}^+)$  is qualitatively similar to  $H_A(\text{Li}^+)$ , whereas the geometry of  $H_{A'A}(\text{Na}^+)$  is qualitatively similar to  $H_A(\text{Na}^+)$ . Although there are otherwise a great number of similarities between  $H_{A'A}(\text{Li}^+)$  and  $H_{A'A}(\text{Na}^+)$ , it is clearer to treat them separately, and we shall start with  $H_{A'A}(\text{Li}^+)$ .

##### A. Analysis of EPR Spectra

$H_{A'A}(\text{Li}^+)$  has a slightly higher thermal stability than  $H_{AA}(\text{Li}^+)$  (Fig. 2). It is therefore a simple matter to eliminate the  $H_{AA}(\text{Li}^+)$  centers and isolate more clearly the  $H_{A'A}(\text{Li}^+)$  EPR spectrum: The crystal is warmed to 275 K for a few minutes and is at the same time (or subsequently) irradiated with light in the  $F$  band, in order to destroy any  $V_{KA}(\text{Li}^+)$  centers that are formed. The  $H_{A'A}(\text{Li}^+)$

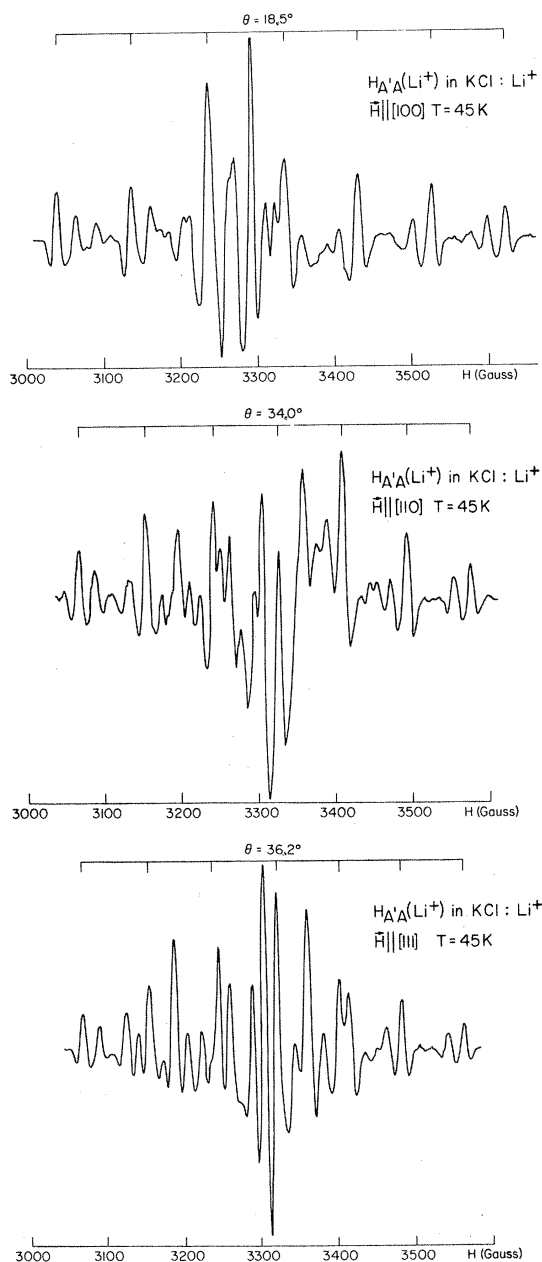


FIG. 5. The  $H_{A'A}(\text{Li}^+)$  EPR spectra in  $\text{KCl}:\text{Li}^+$  at about 45 K. The microwave frequency  $\nu = 9.404$  GHz. The second derivative of the absorption is presented. This figure was redrawn from the experimental spectra.

EPR spectra in  $\text{KCl}:\text{Li}^+$ , taken at about 45 K for three special orientations of the magnetic field  $\vec{H}$ , are shown in Fig. 5. The characteristic 1:2:3:4:3:2:1 seven-line pattern which is observed for all angles, shows that we are dealing with a  $\text{Cl}_2^-$  species whose nuclei are equivalent for all orientations of  $\vec{H}$ . An angular-variation study further shows that the  $\text{Cl}_2^-$  molecular axis lies in a  $\{110\}$  plane and makes an  $(18.5 \pm 0.5)^\circ$  angle with

TABLE II. Classification of the  $H_{A'A}(\text{Li}^+)$  and  $H_{A'A}(\text{Na}^+)$  EPR spectra for three orientations of the static magnetic field  $\vec{H}$ . The  $H_{A'A}(\text{Li}^+)$  center makes an  $18.5^\circ$  angle with  $\langle 100 \rangle$  in a  $\{110\}$  plane, while the  $H_{A'A}(\text{Na}^+)$  center makes a  $11.5^\circ$  angle with  $\langle 110 \rangle$  in a  $\{100\}$  plane.  $\theta$  is the angle between  $\vec{H} \parallel z'$  and the  $H_{A'A}$ -center internuclear axis  $z''$ .

Direction of $\vec{H}$	$H_{A'A}(\text{Li}^+)$ center Angle $\theta$ (deg)	Degeneracy	$H_{A'A}(\text{Na}^+)$ center Angle $\theta$ (deg)	Degeneracy
$\langle 100 \rangle$	18.5	4	33.5	4
	77.5	8	56.5	4
			90	4
$\langle 111 \rangle$	36.2	3	36.9	6
	56.8	6	80.6	6
	73.2	3		
$\langle 110 \rangle$	34.0	4	11.5	2
	59.2	4	53.9	4
	71.5	2	67.0	4
	90	2	78.5	2

$\langle 001 \rangle$ . Table II classifies the number and type of spectra that should be observed for three special orientations of  $\vec{H}$ , and some of the spectra that are readily recognized are indicated in Fig. 5. Thus, the symmetries of  $H_{A'A}(\text{Li}^+)$  and  $H_A(\text{Li}^+)$  are qualitatively the same. In the latter case the  $\text{Cl}_2^-$  internuclear axis makes a  $(26 \pm 1)^\circ$  angle with  $\langle 001 \rangle$  in a  $\{110\}$  plane.<sup>4</sup>

Two differences between  $H_{A'A}(\text{Li}^+)$  and  $H_A(\text{Li}^+)$  should be noted. For  $H_A(\text{Li}^+)$ , the two Cl nuclei 1 and 2 (Fig. 6) are inequivalent for *all* orientations of  $\vec{H}$ , and the  $\text{Cl}_2^-$  molecular bond is bent by about  $8^\circ$ . Furthermore, the  $H_A(\text{Li}^+)$  EPR lines show an angular variation in width and shape which is

caused by unresolved shf structure originating from nuclei 3 and 4 in Fig. 6. No such things are observed in the  $H_{A'A}(\text{Li}^+)$  EPR spectra. Anticipating at this point the proposed model for  $H_{A'A}(\text{Li}^+)$  given in Fig. 6, one can see that if there is any shf at all for  $H_{A'A}(\text{Li}^+)$ , it must come from four Cl nuclei (3, 4, 3', and 4') rather than two. Not only are there many more lines in the shf structure, but its magnitude is expected to be smaller than in the case of  $H_A(\text{Li}^+)$ . Both factors effectively smooth out the structure and anisotropy of the unresolved shf structure.

The  $H_{A'A}(\text{Li}^+)$  EPR spectra were analyzed with a spin Hamiltonian of the form

$$\mathcal{H}/g_0\mu_B = (1/g_0) [g_{\parallel} H_{x''} S_{x''} + g_{\perp} (H_{x''} S_{x''} + H_{y''} S_{y''}) + A_{\parallel} S_{x''} (I_{x''1} + I_{x''2}) + A_{\perp} [S_{x''} (I_{x''1} + I_{x''2}) + S_{y''} (I_{y''1} + I_{y''2})] \quad (4)$$

in which  $z''$  is parallel to the 1-2 internuclear axis. The results are presented in Table III. The perpendicular  $g$  shifts  $\Delta g_{\perp}$  of  $H_A(\text{Li}^+)$  and  $H_{A'A}(\text{Li}^+)$  are comparable. Similarly, the magnitude of the hf interaction in  $H_{A'A}(\text{Li}^+)$  is very nearly equal to the average, over the two Cl nuclei, of the hf interaction of  $H_A(\text{Li}^+)$ . The hf components of  $H_{A'A}(\text{Li}^+)$  are somewhat smaller than those of  $H_{AA}(\text{Li}^+)$  given in Table II. This could indicate<sup>4</sup> a slightly increased  $\text{Cl}_2^-$  internuclear distance for  $H_{A'A}(\text{Li}^+)$ , which in turn would be indicative of a reduced strain field around  $H_{A'A}(\text{Li}^+)$ , compared to  $H_A(\text{Li}^+)$ . The larger  $\Delta g_{\perp}$  also suggest that the optical-absorption bands of  $H_{A'A}(\text{Li}^+)$  will be found at somewhat longer wavelengths than those of  $\text{H}^2$  and  $H_A(\text{Li}^+)$ .<sup>4</sup>

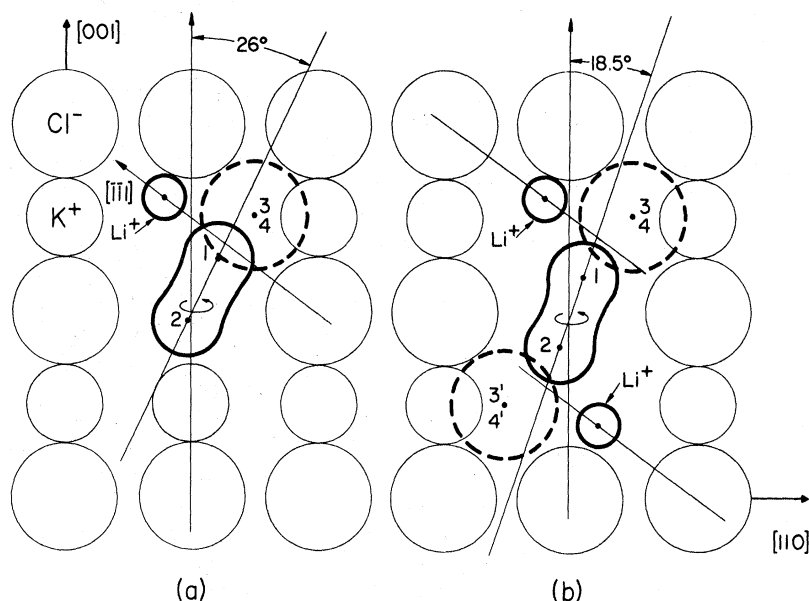


FIG. 6. Schematic representation in a  $\{110\}$  plane of the models of (a) the  $H_A(\text{Li}^+)$  [or  $V_1(\text{Li}^+)$ ] center and (b) the  $H_{A'A}(\text{Li}^+)$  center in  $\text{KCl}:\text{Li}^+$ .



TABLE III. Spin-Hamiltonian parameters of the  $H_A(\text{Li}^+)$  [or  $V_1(\text{Li}^+)$ ] and  $H_{A'A}(\text{Li}^+)$  centers at, respectively, 22 and 45 K. The internuclear axes of both centers are tipped in a  $\{110\}$  plane away from  $\langle 001 \rangle$  (see Fig. 6).

Center	$g_{\parallel}$ $\langle 001 \rangle + \alpha_z$	$g_{\perp}$	$A_{\parallel,2}$ $\langle 001 \rangle + \alpha_{1,2}$	$A_{\perp,2}$	$A_{\parallel,3,4}$	$A_{\perp,3,4}$	$\delta$ (deg)	$\Delta H$	$T_{\text{decay}}$ (K)
$H_A(\text{Li}^+)^a$	$2.0020 \pm 0.0004$	$2.031 \pm 0.002$	$A_{\parallel,1} = 106.5 \pm 0.5$ $A_{\parallel,2} = 96.5 \pm 0.5$	$A_{\perp,1} = 10 \pm 10$ $A_{\perp,2} = 10 \pm 10$	$A_{\parallel,3} \equiv A_{\parallel,4} = 4.2 \pm 0.3$	$A_{\perp,3} \equiv A_{\perp,4} = 1.4 \pm 0.5$	$8 \pm 2$	$3.5 \pm 1$	230
$H_{A'A}(\text{Li}^+)^b$	$2.0020 \pm 0.0005$	$2.031 \pm 0.002$	$A_{\parallel,1} \equiv A_{\parallel,2} = 101.7 \pm 0.3$	$A_{\perp,1} \equiv A_{\perp,2} = 12 \pm 1$			0	$10.5 \pm 1$	283

<sup>a</sup>For  $H_A(\text{Li}^+)$ :  $\alpha_z = 28^\circ \pm 1^\circ$ ;  $\alpha_1 = 30^\circ \pm 1^\circ$ ;  $\alpha_2 = 22^\circ \pm 1^\circ$ . The symmetry axes of  $\vec{A}_3$  and  $\vec{A}_4$  are roughly perpendicular to one another. The 3.5-G linewidth is the reduced linewidth (see Ref. 4).

<sup>b</sup>For  $H_{A'A}(\text{Li}^+)$ :  $\alpha_z \equiv \alpha_1 \equiv \alpha_2 = 18.5^\circ \pm 0.5^\circ$ . The 10.5-G linewidth is believed to originate primarily from unresolved sif interaction with nuclei 3, 4, 3', and 4' shown in Fig. 6.

### B. Model for $H_{A'A}(\text{Li}^+)$ Center

The proposed model for the  $H_{A'A}(\text{Li}^+)$  center is shown schematically in a  $\{110\}$  plane in Fig. 6(b). It is based on the following observations:

(a)  $H_{A'A}(\text{Li}^+)$  is observable only in strongly doped  $\text{KCl}:\text{Li}^+$ , indicating that very likely two  $\text{Li}^+$  ions are involved. (b)  $H_{A'A}(\text{Li}^+)$  is formed when  $H_A(\text{Li}^+)$  and  $H_{AA}(\text{Li}^+)$  decay, i. e.,  $H_{A'A}(\text{Li}^+)$  is very probably an interstitial center. (c)  $H_{A'A}(\text{Li}^+)$  is very likely a neutral center. (d)  $H_{A'A}(\text{Li}^+)$  contains a  $\text{Cl}_2^-$  molecule ion whose nuclei are equivalent for all orientations of  $\vec{H}$  and whose molecular axis makes an  $18.5^\circ$  angle with  $\langle 001 \rangle$  in a  $\{110\}$  plane.

It is difficult to construct a plausible model for the  $H_{A'A}(\text{Li}^+)$  center involving two  $\text{Li}^+$  ions which are nn of each other, and satisfying the above observations. On the other hand, the proposed model as depicted in Fig. 6(b), involving two  $\text{Li}^+$  ions which are nnn of each other, accounts very straightforwardly for all the experimental observations,<sup>22</sup> including the motional effects described below in Sec. V C.

The great similarity between  $H_A(\text{Li}^+)$  and  $H_{A'A}(\text{Li}^+)$  is obvious from Fig. 6. It was proposed that the specific  $H_A(\text{Li}^+)$ -center geometry was connected with the  $\langle 111 \rangle$  off-center displacement of the small  $\text{Li}^+$  ion in  $\text{KCl}$ .<sup>4</sup> After forming the  $H_A(\text{Li}^+)$  center the  $\text{Li}^+$  is displaced along some direction in a  $\{110\}$  plane, but not necessarily along  $\langle 111 \rangle$ . Similarly, the two nnn  $\text{Li}^+$  ions in  $H_{A'A}(\text{Li}^+)$  are believed to be displaced in opposite senses (also not necessarily along  $[\bar{1}\bar{1}1]$  in the same  $(110)$  plane, as depicted in Fig. 6. This figure is also very helpful in explaining the smaller tipping angle of  $H_{A'A}(\text{Li}^+)$  compared to  $H_A(\text{Li}^+)$  ( $18.5^\circ$  vs  $26^\circ$ ): The  $\text{K}^+$  on the other side of the  $\text{Cl}_2^-$  is replaced by a second off-center  $\text{Li}^+$  ion, making more room for the  $\text{Cl}_2^-$  in a direction that lies closer to the  $[001]$  direction. Again the reduced strain field may be the cause of the increased thermal stability of  $H_{A'A}(\text{Li}^+)$  compared to  $H_A(\text{Li}^+)$ .

### C. Motional Effects in $H_{A'A}(\text{Li}^+)$

Inspection of the proposed  $H_{A'A}(\text{Li}^+)$ -center model in Fig. 6(b) shows that  $H_{A'A}(\text{Li}^+)$ , in contrast to the  $H_{AA}$  center, is not a rigid center. The  $\text{Cl}_2^-$  molecule ion possesses four equivalent orientations which it can occupy around a given  $\langle 001 \rangle$  axis (the  $\text{Li}^+-\text{Li}^+$  axis if their off-center displacement is neglected for a moment). If sufficiently thermally activated, the  $\text{Cl}_2^-$  could jump among these four equivalent positions, and  $H_{A'A}(\text{Li}^+)$  would exhibit a restricted motion. Actually, this is precisely what happens. If the EPR spectra are studied as a function of temperature, line broadening is observed above 59 K. That this is a lifetime broadening brought about by a thermally activated restricted motion of

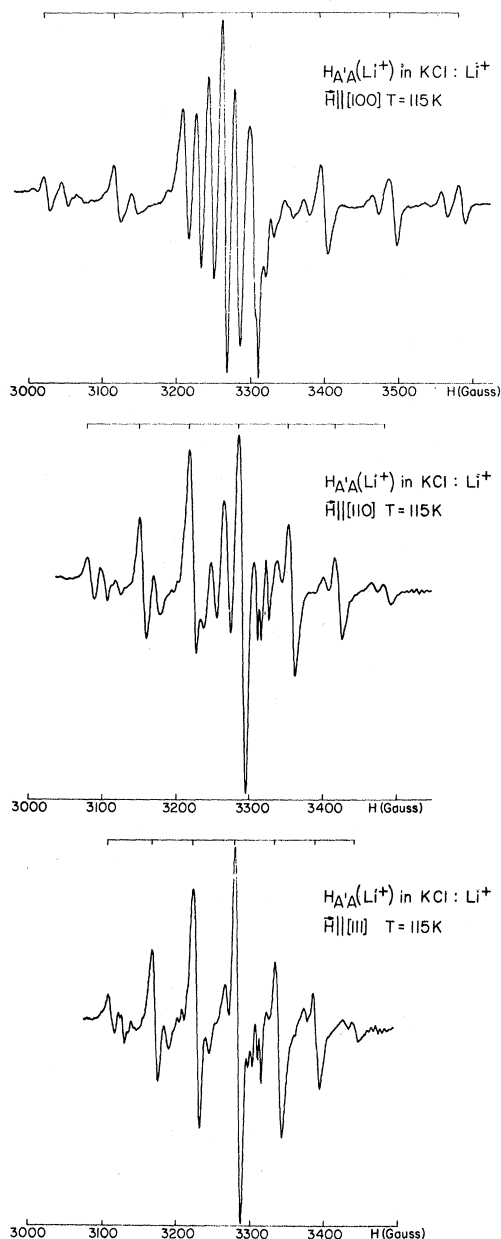


FIG. 7. Motionally averaged  $H_{A'A}(Li^+)$ -center EPR spectra in  $KCl:Li^+$  observed at 115 K. The microwave frequency  $\nu = 9.273$  GHz. The first derivative of the absorption is recorded. Small traces of  $H_{AA}(Li^+)$  are still visible in the  $\langle 111 \rangle$  and  $\langle 110 \rangle$  spectra.

$H_{A'A}(Li^+)$  is indicated by the fact that at 115 K an averaged, but still anisotropic,  $H_{A'A}(Li^+)$  EPR spectrum can be recorded. Above this temperature the lines broaden again. The motionally averaged EPR spectra are shown in Fig. 7 for three special orientations of  $\vec{H}$ . As far as the line positions are concerned, the averaging is complete, but from the point of view of the line shape, the averaging is not yet complete for

$\vec{H} \parallel \langle 110 \rangle$  and  $\vec{H} \parallel \langle 111 \rangle$ . In going from the inner to the outer lines, the distribution of the peak intensities drops faster than the standard 1:2:3:4:3:2:1 distribution of  $Cl_2^-$ . However, because of the large hf anisotropy, the outer lines are averaged over larger magnetic field intervals than the inner lines, and motional averaging and subsequent motional narrowing occurs earlier (i.e., at lower temperatures or lower motional frequencies) for the inner than for the outer lines. Furthermore, rapid motion influences the relaxation behavior of the various hf components differently.<sup>23,24</sup> We will not concern ourselves here with this aspect of the  $H_{A'A}(Li^+)$ -center motion.<sup>25</sup>

Each spectrum in Fig. 7 can be analyzed for the first-order hf separation  $\langle K \rangle$  and the  $g$  factor  $\langle g \rangle$ . The results are given in Table IV. It will be shown that these  $\langle K \rangle$ 's and  $\langle g \rangle$ 's are straightforwardly derived from the  $H_{A'A}(Li^+)$  spin-Hamiltonian parameters in Table III, when it is assumed that the  $Cl_2^-$  executes a rapid pyramidal jumping motion around  $\langle 001 \rangle$  in the four  $\{110\}$  half-planes.

Spin Hamiltonian (4) is expressed in the  $(x'', y'', z'')$  coordinate system of the  $H_{A'A}(Li^+)$  center itself, but the experimental spectra in Fig. 7 represent motionally averaged spectra with respect to a given direction of  $\vec{H}$ . Therefore (4) is reexpressed in a  $(x', y', z')$  coordinate system<sup>23,24</sup> for which  $z' \parallel \vec{H}$  always (Fig. 8):

$$\begin{aligned} \mathcal{H}_i / g_0 \mu_B = & (1/g_0) [(g_{\parallel} - g_{\perp}) \cos^2 \theta_i + g_{\perp}] H S_{z'} \\ & + (1/g_0) (g_{\parallel} - g_{\perp}) \sin \theta_i \cos \theta_i H [S_{x'} \cos \varphi_i + S_{y'} \sin \varphi_i] \\ & + [(A_{\parallel} - A_{\perp}) \cos^2 \theta_i + A_{\perp}] S_{z'} (I_{x',1} + I_{x',2}) \\ & + (A_{\parallel} - A_{\perp}) \sin \theta_i \cos \theta_i S_{z'} [(I_{x',1} + I_{x',2}) \cos \varphi_i \\ & + (I_{y',1} + I_{y',2}) \sin \varphi_i], \quad (5) \end{aligned}$$

in which  $(\theta_i; \varphi_i)$  are the polar coordinates of  $z''$  with respect to  $(x', y', z')$ . The index  $i$  specifies the four possible orientations of  $z''$  with respect to  $\vec{H} \parallel z'$ , and with respect to the laboratory reference frame  $(x, y, z)$  (Fig. 8). Transformed spin Hamiltonian (5) is not complete but should include a number of off-diagonal hf terms. These neglected terms, which can be found in Refs. 23 and 24, are important if one wants to include the total effect of the  $g$  anisotropy on the hf separation. The  $g$  anisotropy is quite small in our case, and the first-order treatment implied by (5) is not only sufficiently accurate but also clearer.

Spin Hamiltonian (5) will now be averaged. This averaging is based on the following three assumptions: (a) The  $Cl_2^-$  molecule ion of  $H_{A'A}(Li^+)$  jumps between the four equivalent, i.e., equally probable, orientations around  $\langle 001 \rangle$  in the  $\{110\}$  planes. (b) The jump time or transit time, i.e., the time

TABLE IV. Comparison between the experimental and calculated values of  $\langle K \rangle$  (in G) and  $\langle g \rangle$  of the motionally averaged  $H_{AA}(\text{Li}^+)$ -center EPR spectra observed at 115 K. The parameters  $\alpha$  and  $\beta$  and the  $(\theta_i; \varphi_i)$  sets over which averaging is performed are also given.

$H \parallel \langle 001 \rangle^a$		$H \parallel \langle 110 \rangle^b$		$H \parallel \langle 111 \rangle^c$		
$\alpha = 0.899$		$\alpha = 0.475$		$\alpha = 0.333$		
$\beta = 0$		$\beta = 0.428$		$\beta = 0.401$		
expt	calc	expt	calc	expt	calc	
$\langle K \rangle$	91.5	92.6	65.7	66.7	54.3	55.1
$\langle g \rangle$	2.0049	2.0049	2.017	2.017	2.020	2.021

<sup>a</sup> $(\theta_i; \varphi_i)$  set:  $(18.5^\circ; 0^\circ)$ ,  $(18.5^\circ; 90^\circ)$ ,  $(18.5^\circ; 180^\circ)$ ,  $(18.5^\circ; 270^\circ)$ .

<sup>b</sup> $(\theta_i; \varphi_i)$  set:  $(34.0^\circ; 23.7^\circ)$ ,  $(59.2^\circ; 11.1^\circ)$ ,  $(59.2^\circ; -11.1^\circ)$ ,  $(34.0^\circ; -23.7^\circ)$ .

<sup>c</sup> $(\theta_i; \varphi_i)$  set:  $(36.2^\circ; 0^\circ)$ ,  $(56.8^\circ; 22.3^\circ)$ ,  $(73.2^\circ; 0^\circ)$ ,  $(56.8^\circ; -22.3^\circ)$ .

in going from one orientation to a neighboring orientation, is negligibly small compared to the lifetime (correlation time) of the  $\text{Cl}_2^-$  in a given orientation. (Actually, the transit time is very likely of the order of the inverse of the lattice vibrational frequencies, i. e., of the order of  $10^{-12}$ – $10^{-14}$  sec. Since the transit time is negligibly small, the actual path of the molecule in transit is also irrelevant. (c) The jump frequency, i. e., the inverse of the correlation time, is higher than the frequency associated with the combined effect of the  $g$  anisotropy [ $\sim (1/g_0) \times (g_{\parallel} - g_{\perp})\mu_B H$ ] and the hf anisotropy [ $\sim (A_{\parallel} - A_{\perp})M_I$ ] With these assumptions the spin Hamiltonian describing the averaged EPR spectra is simply

$$\langle \mathcal{H} \rangle = \frac{1}{4} \sum_{i=1}^4 \frac{\mathcal{H}_i}{g_0 \mu_B}, \quad (6)$$

in which the summation is over the four possible orientations of  $z''$ , as illustrated in Fig. 9(a). Since the  $\text{Cl}_2^-$  is jumping as a whole, the electron-spin and nuclear-spin operators are identical in each orientation of the center. Averaging in (6) thus merely involves averaging of the coefficients of these operators.

Therefore, defining

$$\begin{aligned} \alpha &= \frac{1}{4} \sum_{i=1}^4 \cos^2 \theta_i, \\ \beta &= \frac{1}{4} \sum_{i=1}^4 \sin \theta_i \cos \theta_i \cos \varphi_i, \\ \gamma &= \frac{1}{4} \sum_{i=1}^4 \sin \theta_i \cos \theta_i \sin \varphi_i, \end{aligned} \quad (7)$$

the hf separation  $\langle K \rangle$  (ignoring all  $g$  anisotropy), and the  $g$  factor  $\langle g \rangle$ , resulting from  $\langle \mathcal{H} \rangle$  are<sup>24</sup>

$$\begin{aligned} \langle K \rangle^2 &= [(A_{\parallel} - A_{\perp})\alpha + A_{\perp}]^2 + (A_{\parallel} - A_{\perp})^2(\beta^2 + \gamma^2), \\ \langle g \rangle^2 &= [(g_{\parallel} - g_{\perp})\alpha + g_{\perp}]^2 + (g_{\parallel} - g_{\perp})^2(\beta^2 + \gamma^2). \end{aligned} \quad (8)$$

The pyramidal jumping motion takes place around

$\langle 001 \rangle$ , which we choose as the  $z$  axis of a  $(x, y, z)$  laboratory coordinate system. The  $\alpha$ ,  $\beta$ , and  $\gamma$  should be evaluated in this frame and we choose, e. g.,  $x$  such that it lies in one of the four possible  $(z, z'')$  planes [see Fig. 9(a)]. With this choice of axes one finds that  $\gamma = 0$ . Furthermore it is easy to demonstrate that

$$\alpha = \cos^2 \theta \cos^2 \theta'' + \frac{1}{2} \sin^2 \theta \sin^2 \theta''. \quad (9)$$

Only for a few special orientations of  $\vec{H}$  can closed expressions for  $\beta$  be derived in the  $(x, y, z)$  frame (e. g., for  $\theta = 0^\circ$ ,  $\beta = 0$ ), and in general it is easier to calculate the  $\beta$  numerically using the  $(\theta_i; \varphi_i)$  values. In the latter case one can again accomplish  $\gamma = 0$ , if one chooses the  $(z', x') \equiv (z', z)$  plane such that it either coincides with a (1, 3) or (2, 4) plane (Fig. 9), or is perpendicular to such a plane.

In the special cases that we treat, these conditions can be fulfilled.

As a nontrivial example, the case of  $\vec{H} \parallel \langle 111 \rangle$ , i. e.,  $\theta' = 35.26^\circ$ , will be treated in some detail. In this case, the pyramidal motions around  $[001]$ ,  $[010]$ , and  $[100]$  are the same with respect to  $\vec{H}$ , and only one EPR spectrum should be observed for this orientation. Figure 7 shows that this is indeed true. The four  $(\theta_i; \varphi_i)$  sets involved in the averaging are  $(36.2^\circ; 0^\circ)$ ,  $(56.8^\circ; 22.3^\circ)$ ,  $(73.2^\circ; 0^\circ)$ , and  $(56.8^\circ; -22.3^\circ)$ . Hence, from (7),

$$\beta = 0.401, \quad \alpha = 0.333. \quad (10)$$

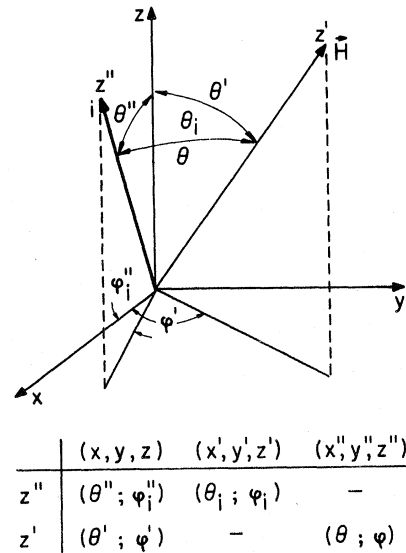


FIG. 8. Various coordinate systems and definition of the polar coordinates, used in the transformation of spin Hamiltonian (4) and the description of the motions of the  $H_{AA}(\text{Na}^+)$  and  $H_{AA}(\text{Li}^+)$  centers. Note that  $\theta_i = \theta$  but  $\varphi_i \neq \varphi$ .

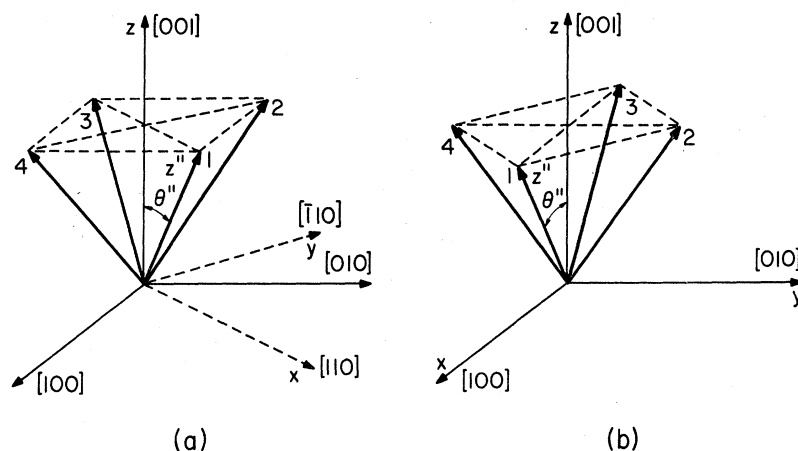


FIG. 9. Schematic representation of the four orientations of the pyramidal motion of (a) the  $H_{A'A}(\text{Li}^+)$  center around  $\langle 110 \rangle$  in the  $\{110\}$  planes  $\{z''\}$  was chosen to lie in the  $(z, x)$  plane with  $z \parallel [001]$  and  $x \parallel [110]$  and (b) the  $H_{A'A}(\text{Na}^+)$  center around  $\langle 001 \rangle$  in the  $\{100\}$  planes  $\{z''\}$  was chosen to lie in the  $(z, x)$  plane with  $z \parallel [001]$  and  $x \parallel [100]$ .

The latter also follows immediately from (9). Using (8) and (10) and the Hamiltonian parameters of Table III, one calculates

$$\langle K \rangle = 55.1 \text{ G},$$

$$\langle g \rangle = 2.021,$$

which are very close to the experimental values of Table IV. This table shows the  $\alpha$  and  $\beta$  values for the other orientations of  $\vec{H}$  and the  $(\theta_i; \varphi_i)$  sets used for the averaging. The agreement between the experimental and calculated  $\langle K \rangle$  and  $\langle g \rangle$  values is quite good as Table IV shows. This good agreement [which would probably be improved if off-diagonal hf terms, which were neglected in (5), were taken into account] leaves little doubt that the  $H_{A'A}(\text{Li}^+)$  center does indeed exhibit a restricted pyramidal jumping motion around  $\langle 001 \rangle$  in the  $\{110\}$  planes, as shown in Fig. 9(a).

The two  $\text{Li}^+$  ions are, as indicated in Fig. 6(b), displaced substantially from the normal-lattice positions. This therefore implies that when the  $\text{Cl}_2^-$  in  $H_{A'A}(\text{Li}^+)$  jumps from one  $\{110\}$  plane to another  $\{110\}$  plane, the two  $\text{Li}^+$  ions must also and simultaneously jump from one  $\{110\}$  plane to another. In other words, the pyramidal jumping motion of the  $\text{Cl}_2^-$  in  $H_{A'A}(\text{Li}^+)$  implies a cooperative jumping motion of the two  $\text{Li}^+$  ions. Thus the possibility in principle exists that  $H_{A'A}({}^7\text{Li}^+)$  (in normal  $\text{KCl}:\text{Li}^+$  crystals since  ${}^7\text{Li}$  is 92.6% abundant) and  $H_{A'A}({}^6\text{Li}^+)$  (in  ${}^6\text{Li}$ -enriched  $\text{KCl}:\text{Li}^+$  crystals since  ${}^6\text{Li}$  is 7.4% abundant) may show, at the same temperature, a difference in the frequency of their respective pyramidal jumping motions. However, very careful measurements are probably needed to establish such a difference, if it is measurable at all.

The pyramidal jumping motion of  $H_{A'A}(\text{Li}^+)$  is clearly thermally activated, and it is believed that at sufficiently low temperatures each  $H_{A'A}(\text{Li}^+)$  freezes into a particular orientation. Excitation

with polarized light at low temperatures, with the purpose of obtaining an anisotropy in the distribution of the  $H_{A'A}(\text{Li}^+)$  orientations, could in principle confirm this. However, such measurements were not attempted.

#### VI. $H_{A'A}(\text{Na}^+)$ CENTER

After having produced  $H_{AA}(\text{Na}^+)$  (see Sec. III), the  $H_{A'A}(\text{Na}^+)$  center can be isolated by a warm-up to 150 K for a few minutes and a subsequent elimination of the  $\text{Cl}_2^- V_K$  centers through an optical excitation of the  $F$  centers. Except for a difference in geometry, the properties of  $H_{A'A}(\text{Na}^+)$  and  $H_{A'A}(\text{Li}^+)$  are very similar. Therefore, the reasons for ascribing the  $H_{A'A}(\text{Na}^+)$  EPR spectrum to a model involving a  $\text{Cl}_2^-$  in a single-negative-ion vacancy and two nnn  $\text{Na}^+$  ions [Fig. 11(b)] will not be repeated. We will only concentrate on the difference in geometry between the two centers and show that the  $\text{Cl}_2^-$  molecular axis in  $H_{A'A}(\text{Na}^+)$  makes an  $11.5^\circ$  angle with  $\langle 110 \rangle$  in a  $\{001\}$  plane, as shown in Fig. 6(b), in contrast to  $H_{A'A}(\text{Li}^+)$  which makes an  $18.5^\circ$  angle with  $\langle 001 \rangle$  in a  $\{110\}$  plane.

This model for  $H_{A'A}(\text{Na}^+)$  implies that it is not a rigid center, but that the  $\text{Cl}_2^-$  can in principle, perform a pyramidal jumping motion around  $\langle 001 \rangle$ . Such a thermally activated restricted motion is indeed observed experimentally for  $H_{A'A}(\text{Na}^+)$  at 150 K.

A reverse analysis will be performed: The  $H_{A'A}(\text{Na}^+)$ -center geometry will be derived partly from the motionally averaged  $H_{A'A}(\text{Na}^+)$  EPR spectra. These spectra, which are shown in Fig. 10, were recorded at 150 K, i.e., just below the decay temperature of  $H_{A'A}(\text{Na}^+)$ . For the same reasons as given in the case of  $H_{A'A}(\text{Li}^+)$ , the 1:2:3:4:3:2:1 peak-intensity ratios are not obtained for the  $\vec{H} \parallel \langle 110 \rangle$  and  $\vec{H} \parallel \langle 111 \rangle$   $H_{A'A}(\text{Na}^+)$  spectra. The experimentally determined first-order hf separations  $\langle K \rangle$  and the  $g$  factors  $\langle g \rangle$  are

TABLE V. Comparison between the experimental and calculated values of  $\langle K \rangle$  (in G) and  $\langle g \rangle$  of the motionally averaged  $H_{A'A}(Na^+)$  EPR spectrum observed at 150 K. The parameters  $\alpha$  and  $\beta$  and the  $(\theta_i; \varphi_i)$  sets over which is the averaging is performed are also given.

$H \parallel \langle 001 \rangle^a$		$H \parallel \langle 110 \rangle^b$		$H \parallel \langle 111 \rangle^c$		
$\alpha = 0.695$		$\alpha = 0.424$		$\alpha = 0.333$		
$\beta = 0$		$\beta = 0.272$		$\beta = 0.256$		
expt	calc	expt	calc	expt	calc	
$\langle K \rangle$	77.4 <sup>d</sup>	(77.4) <sup>d</sup>	56.4	58.1	49.3	50.1
$\langle g \rangle$	2.011	2.010	2.018	2.018	2.020	2.020

<sup>a</sup> $(\theta_i; \varphi_i)$  set:  $(33.5^\circ; 0^\circ)$ ,  $(33.5^\circ; 90^\circ)$ ,  $(33.5^\circ; 180^\circ)$ ,  $(33.5^\circ; 270^\circ)$ .

<sup>b</sup> $(\theta_i; \varphi_i)$  set:  $(11.5^\circ; 0^\circ)$ ,  $(53.9^\circ; 43.1^\circ)$ ,  $(78.5^\circ; 0^\circ)$ ,  $(53.9^\circ; -43.1^\circ)$ .

<sup>c</sup> $(\theta_i; \varphi_i)$  set:  $(36.9^\circ; 40.6^\circ)$ ,  $(36.9^\circ; -40.6^\circ)$ ,  $(80.6^\circ; 23.4^\circ)$ ,  $(80.6^\circ; -23.4^\circ)$ .

<sup>d</sup>Used to determine the  $11.5^\circ \pm 1^\circ$  tipping angle with respect to  $\langle 110 \rangle$ .

summarized in Table V.

The reverse analysis will be performed with the following assumptions: (a) Whatever the orientation of the  $Cl_2^-$  in  $H_{A'A}(Na^+)$ , experience with  $H_A(Li^+)$  (see Table III) indicates that the hf parameters will be close to  $A_{||} = 105$  G and  $A_{\perp} = 14$  G, i. e., close to the average of the  $H_A(Na^+)$  hf parameters. (b) The  $Cl_2^-$  of  $H_{A'A}(Na^+)$  exhibits a pyramidal jumping motion around  $\langle 100 \rangle$  among the four equivalent orientations in the  $\{100\}$  planes. The geometry of this motion is shown schematically in Fig. 9(b). Formulas (8) for  $\langle K \rangle$  and  $\langle g \rangle$ , and the expression for  $\alpha$ ,  $\beta$ , and  $\gamma$  as given in (7) and (9), apply for  $H_{A'A}(Na^+)$ . With the choice of axes  $(x, y, z)$  in Fig. 9(b), one finds again that  $\gamma = 0$ . The parameter  $\beta$  is most conveniently determined numerically using the  $(\theta_i; \varphi_i)$  sets.

The angle  $\theta''$  that the  $Cl_2^-$  axis makes with  $\langle 001 \rangle$  can be determined from  $\langle K \rangle = 77.4$  G, which is the value of the hf separation of the  $\vec{H} \parallel \langle 100 \rangle$  EPR spectrum. It is found by solving

$$\langle K \rangle = (A_{||} - A_{\perp}) \cos^2 \theta'' + A_{\perp},$$

which is obtained from (8), noting that for  $\vec{H} \parallel \langle 100 \rangle$ ,  $\alpha = \cos^2 \theta''$  and  $\beta = \gamma = 0$ . This yields  $\theta'' = 33.5^\circ$ , i. e., the  $Cl_2^-$  molecular axis makes a  $11.5^\circ$  angle with  $\langle 110 \rangle$  in a  $\{100\}$  plane. (Actually, at this point in the analysis it is not known, of course, that  $\theta''$  lies in a  $\{100\}$  plane; it could also lie in a  $\{110\}$  plane. However, as one can verify, with the latter assumption, no agreement between the experimental and calculated values of  $\langle K \rangle$  and  $\langle g \rangle$  is obtained for  $\vec{H} \parallel \langle 111 \rangle$  and  $\vec{H} \parallel \langle 110 \rangle$ .) The fact that this  $11.5^\circ$  angle for  $H_{A'A}(Na^+)$  is, within the accuracy of the analysis, twice as big as the  $5.7^\circ$  angle found for  $H_A(Na^+)$ , which involved only one  $Na^+$  impurity ion, is very probably accidental.

With the knowledge of this  $11.5^\circ$  tipping angle,

the  $\langle K \rangle$  and  $\langle g \rangle$  values of the motionally averaged EPR spectra, observed when  $\vec{H} \parallel \langle 111 \rangle$  and  $\vec{H} \parallel \langle 110 \rangle$ , are easily calculated. In calculating the  $\langle g \rangle$  values, the very reasonable assumption was made that  $g_{||} = 2.0018$ . The  $g_{\perp}$  parameter was then determined by selecting the value that gave the best calculated  $\langle g \rangle$  values. The results are given in Table V. This table also gives the  $\alpha$  and  $\beta$  values and the  $(\theta_i; \varphi_i)$  sets used in the averaging.

The agreement shown in Table V is quite good,

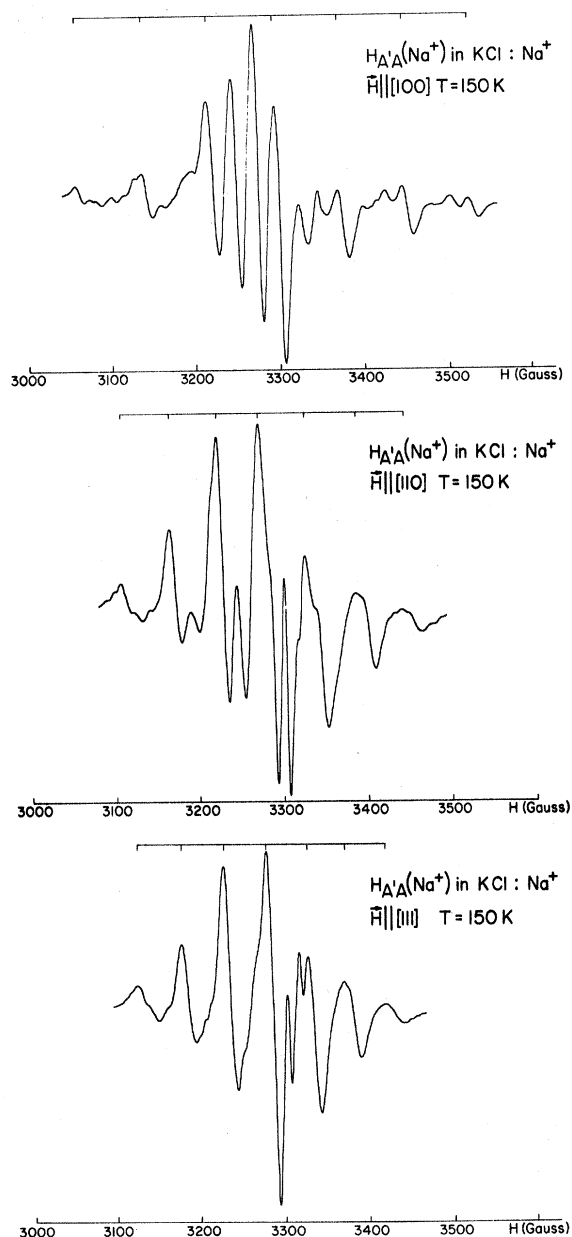


FIG. 10. Motionally averaged  $H_{A'A}(Na^+)$ -center EPR spectra in  $KCl:Na^+$  observed at 150 K. The first derivative of the absorption is presented.

TABLE VI. Spin-Hamiltonian parameters of the  $H_A(\text{Na}^\bullet)$  [or  $V_1(\text{Na}^\bullet)$ ] and  $H_{A'A}(\text{Na}^\bullet)$  centers at, respectively, 35 and <77 K. The symmetry axes of both centers are tipped in a  $\{100\}$  plane away from  $\langle 110 \rangle$  (see Fig. 11). The  $H_{A'A}(\text{Na}^\bullet)$  parameters were partly derived from the motionally averaged EPR spectra observed at 150 K.

Center	$g_z''$ $\langle 110 \rangle + \alpha_g$	$g_x''$ $\langle 001 \rangle$	$g_y''$	$A_{\parallel 1,2}$ $\langle 110 \rangle + \alpha_{1,2}$	$A_{\perp 1,2}$	$A_{\parallel 3,4}$ $\langle 110 \rangle + \alpha_{3,4}$	$A_{\perp 3,4}$	$\delta_{1,2}$ (deg)	$\Delta H$	$T_{\text{decay}}$ (K)
$H_A(\text{Na}^\bullet)^a$	2.0018 $\pm 0.0003$	2.024 $\pm 0.001$	2.027 $\pm 0.001$	$A_{\parallel 1} = 109.1$ $\pm 0.1$ $A_{\parallel 2} = 101.1$ $\pm 0.1$	$A_{\perp 1} = 14$ $\pm 4$ $A_{\perp 3} = 14$ $\pm 4$	$A_{\parallel 3} = 13.7$ $\pm 0.1$ $A_{\parallel 4} = 3.1$ $\pm 0.1$	$A_{\perp 3} = 4.6$ $\pm 0.5$ $A_{\perp 4} = 1.3$ $\pm 0.5$	4.5 $\pm 1$	1.8 $\pm 0.1$	110
$H_{A'A}(\text{Na}^\bullet)^b$	2.0018	2.029		$A_{\parallel 1} \equiv A_{\parallel 2}$ $= 105.2$	$A_{\perp 1} \equiv A_{\perp 2}$ $= 14$	$A_{\parallel 3} \equiv A_{\parallel 4}^c$	$A_{\perp 3} \equiv A_{\perp 4}^c$	0 <sup>d</sup>	...	158

<sup>a</sup>For  $H_A(\text{Na}^\bullet)$ :  $\alpha_g = \alpha_3 = \alpha_4 = 5.7^\circ \pm 0.3^\circ$ ;  $\alpha_1 = 3.5^\circ \pm 0.6^\circ$ ;  $\alpha_2 = 8.0^\circ \pm 0.6^\circ$  (from Refs. 3 and 13).

<sup>b</sup>For  $H_{A'A}(\text{Na}^\bullet)$ :  $\alpha_g \equiv \alpha_1 \equiv \alpha_2 = 11.5^\circ \pm 1^\circ$ .

<sup>c</sup>The symmetry of the  $H_{A'A}(\text{Na}^\bullet)$  suggest such an interac-

tion, but it was not resolved in our experiments. Therefore,  $\alpha_3$ ,  $\alpha_4$ , and the linewidth  $\Delta H$  could not be determined. <sup>d</sup>The symmetry of  $H_{A'A}(\text{Na}^\bullet)$  suggests that  $\delta_{1,2} \equiv 0^\circ$ .

and this not only indicates that our choice of  $A_{\parallel}$  and  $A_{\perp}$  (Table VI) was very reasonable, but it also proves that the pyramidal jumping motion is indeed taking place around  $\langle 001 \rangle$  in  $\{100\}$  planes. By analogy with  $H_{A'A}(\text{Li}^\bullet)$  there is also very likely a cooperative motion of the two  $\text{Na}^\bullet$  ions around  $\langle 001 \rangle$  in  $\{100\}$  planes, though probably less pronounced than for the two  $\text{Li}^\bullet$  ions in  $H_{A'A}(\text{Li}^\bullet)$ .

At lower temperatures, where the  $\text{Cl}_2^-$  of the  $H_{A'A}(\text{Na}^\bullet)$  center is either frozen in, or jumping with a frequency too low to result in excessive lifetime broadening of the EPR lines, an anisotropic  $H_{A'A}(\text{Na}^\bullet)$  EPR spectrum should be observed corresponding to the  $H_{A'A}(\text{Na}^\bullet)$  classification of Table II. Such a spectrum would probably also show a shf structure originating from the nuclei of ions 3 and 4 shown in Fig. 11. However, the low concentration of the  $H_{A'A}(\text{Na}^\bullet)$  center, together with the somewhat lower sensitivity of the spectrometer used in the experiments below 77 K, resulted in

very weak EPR spectra which were very difficult to analyze. In particular, the  $11.5^\circ$  tipping angle could not be determined directly through an angular variation study. However, at 77 K the anisotropic spectrum is observable, though the lines are very strongly lifetime broadened by the pyramidal jumping motion. The following parameters could nevertheless be determined:

$$K_{\text{expt}}(11.5^\circ) = (103.3 \pm 1) \text{ G} \quad \text{from } \vec{H} \parallel \langle 110 \rangle,$$

$$K_{\text{expt}}(36.9^\circ) = (84.2 \pm 0.3) \text{ G} \quad \text{from } \vec{H} \parallel \langle 111 \rangle,$$

$$g_{\text{expt}}(36.9^\circ) = 2.012 \pm 0.002.$$

Using (2) and the parameters of Table VI these values can be calculated. One finds

$$K_{\text{calc}}(11.5^\circ) = 103.3 \text{ G},$$

$$K_{\text{calc}}(36.9^\circ) = 84.0 \text{ G},$$

$$g_{\text{calc}}(36.9^\circ) = 2.012.$$

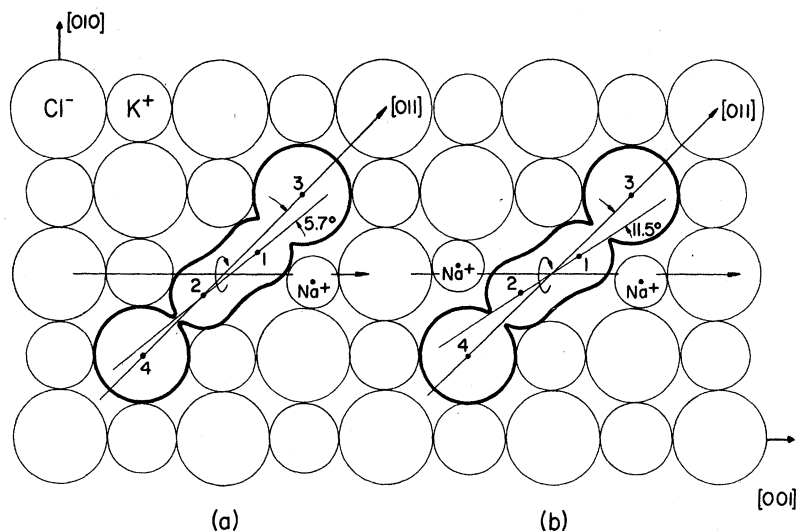


FIG. 11. Schematic models of (a) the  $H_A(\text{Na}^\bullet)$  [or  $V_1(\text{Na}^\bullet)$ ] center and (b) the  $H_{A'A}(\text{Na}^\bullet)$  center in  $\text{KCl}:\text{Na}^\bullet$ .

This agreement further substantiates the  $H_{A'A}(Na^+)$  parameters of Table VI, and the geometry of  $H_{A'A}(Na^+)$  as depicted in Fig. 11.

Finally, Fig. 11 suggests why the tipping angle for  $H_{A'A}(Na^+)$  is larger than for  $H_A(Na^+)$ : The second  $Na^+$  creates more room for the  $Cl_2^-$  in a direction closer to  $\langle 001 \rangle$ , i. e., farther away from  $\langle 011 \rangle$ .

## VII. CONCLUDING REMARKS

We have shown that interstitial Cl atoms can be stabilized to a higher temperature by nn and nnn pairs of  $Na^+$  or  $Li^+$  impurity ions in strongly doped KCl. That this is so should, of course, not be surprising after it had been established<sup>3,4</sup> that single  $Na^+$  and  $Li^+$  ions are very effective in stabilizing interstitial Cl atoms. It is reasonable that two should do better than one in this respect. The smaller size of the  $Na^+$  and  $Li^+$  ions allows them to be pushed farther away from their lattice position, by the interstitial, than the  $K^+$  ions. This results in more room for the  $Cl_2^-$  and a reduction in both overlap and repulsive forces between the  $Cl_2^-$  and the surroundings. In other words, there is a progressive reduction in strain within and around the interstitial center when one or two of the immediate  $K^+$  neighbors are replaced by  $Na^+$  or  $Li^+$  ions. The experimental results definitely suggest a correlation between reduced strain and higher thermal stability:  $H_{AA}$  and  $H_{A'A}$  are more stable than  $H_A$ , which in turn is more stable than the  $H$  center; also, the  $Li^+$ -trapped interstitial centers have a considerably higher thermal stability than the corresponding  $Na^+$ -associated centers. This correlation extends to the spin-Hamiltonian parameters, in particular, to  $g_1$  and  $A_{||}$ . For the  $H$ -type centers described in this paper, an increase in  $\Delta g_1 = g_1 - g_0$  is always accompanied by a reduction in  $A_{||}$ , and such a behavior was interpreted<sup>4</sup> as being indicative of a small increase in the  $Cl_2^-$  internuclear distance, i. e., as a reduction of the strain within the center. Since the latter should reflect the strain around the center, higher thermal stability should be correlated with a larger  $\Delta g_1$  or smaller  $A_{||}$ . The experimental results do indeed show such a correlation.

The straightforwardness with which the experimental observations can be explained with the proposed  $H_{AA}$  and  $H_{A'A}$  models as depicted in Figs. 4, 6, and 11, leaves little doubt that these schematic models are correct. A particularly satisfying aspect in this connection is, on the one hand, the absence of any evidence of motion for the  $H_{AA}$  cen-

ters, and on the other hand, the observation of the restricted pyramidal jumping motions around  $\langle 001 \rangle$  for both  $H_{A'A}(Na^+)$  and  $H_{A'A}(Li^+)$ , as allowed by their proposed models.

The direct experimental observation of the pyramidal motions of  $H_{A'A}(Na^+)$  and  $H_{A'A}(Li^+)$  is quite interesting in connection with the study of the motions exhibited by the  $H_A(Na^+)$  and  $H_A(Li^+)$  centers. It was shown that  $H_A(Na^+)$  exhibits two distinct motions.<sup>3</sup> One of these, called the restricted interstitial jump, consists of the interstitial 1 in Fig. 11(a) being exchanged between ions 2 and 3. This restricted jump is directly observable in the EPR spectrum through a collapsing of certain four-line manifolds in the shf structure as the temperature is raised. However, in order to explain the further averaged  $H_A(Na^+)$  EPR spectrum observed at 77 K, one had to accept the existence of a second motion. It was proposed that this second motion was a pyramidal jumping motion of the  $Cl_2^-$  around  $\langle 001 \rangle$ , rather than a more unrestricted motion of the interstitial around the  $Na^+$  impurity. The pyramidal motion as such, however, was not directly observable in the EPR spectra. The direct observation of the pyramidal jumping motion around  $\langle 001 \rangle$  for  $H_{A'A}(Na^+)$ , and the great similarity in structure between  $H_{A'A}(Na^+)$  and  $H_A(Na^+)$ , leaves little doubt that this type of motion does indeed occur as a distinct motion in the  $H_A(Na^+)$  center. Actually, the pyramidal jumping motion is essentially the same as the "60°-jump" motion that the  $Cl_2^-$  molecule ion of the  $H$  center performs between the six  $\langle 110 \rangle$  orientations above 10.9 K.<sup>2,26</sup> But the presence of one  $Na^+$  for  $H_A(Na^+)$ , or two  $Na^+$ 's for  $H_{A'A}(Na^+)$ , imposes a preferential axis along a specific  $\langle 001 \rangle$  direction, and the "60° jumps" (which, because of the tilting away from  $\langle 110 \rangle$ , are really, respectively, 53.2° and 45.9° jumps) become restricted to the four possibilities around a given  $\langle 001 \rangle$ .

The pyramidal motion around  $\langle 001 \rangle$  is also a distinct motion occurring in the  $H_A(Li^+)$  center. However, the analysis of the  $H_A(Li^+)$ -center motions, together with an attempt at a more quantitative comparison of the various pyramidal motions, will be presented separately in a forthcoming paper.<sup>27</sup>

## ACKNOWLEDGMENTS

The author wishes to thank P. H. Yuster for reading the manuscript and for helpful comments, E. L. Yasaitis for assistance with the low-temperature EPR measurements, and E. Hutchinson for growing the crystals.

\*Work performed under the auspices of the U. S. Atomic Energy Commission.

<sup>1</sup>W. Känzig and T. O. Woodruff, J. Phys. Chem. Solids **9**, 70 (1958).

<sup>2</sup>C. J. Delbecq, J. L. Kolopus, E. L. Yasaitis, and P. H. Yuster, Phys. Rev. **154**, 866 (1967).

<sup>3</sup>C. J. Delbecq, E. Hutchinson, D. Schoemaker, E. L. Yasaitis, and P. H. Yuster, Phys. Rev. **187**,

1103 (1969).

<sup>4</sup>D. Schoemaker and J. L. Kolopus, Phys. Rev. B **2**, 1148 (1970).

<sup>5</sup>G. Guiliani, Phys. Rev. B **2**, 464 (1970).

<sup>6</sup>N. Itoh and M. Saidoh, Phys. Status Solidi **33**, 649 (1969); M. Saidoh and N. Itoh, Phys. Letters **31A**, 68 (1970).

<sup>7</sup>G. J. Dienes, R. D. Hatcher, and R. Smoluchowski, Phys. Rev. **157**, 692 (1967); R. D. Hatcher, W. D. Wilson, R. Smoluchowski, and G. J. Dienes, Bull. Am. Phys. Soc. **14**, 324 (1969).

<sup>8</sup>N. E. Byer and H. S. Sack, J. Phys. Chem. Solids **29**, 677 (1968).

<sup>9</sup>T. G. Castner and W. Känzig, J. Phys. Chem. Solids **3**, 178 (1957); T. O. Woodruff and W. Känzig, *ibid.* **5**, 268 (1958).

<sup>10</sup>C. J. Delbecq, B. Smaller, and P. H. Yuster, Phys. Rev. **111**, 1235 (1958); C. J. Delbecq, W. Hayes, and P. H. Yuster, *ibid.* **121**, 1043 (1961).

<sup>11</sup>D. Schoemaker, in Proceedings of the International Symposium on Color Centers in Alkali Halides, University of Illinois, Urbana, 1965, Abstract No. 167 (unpublished).

<sup>12</sup>I. L. Bass and R. L. Mieher, Phys. Rev. **175**, 421 (1968).

<sup>13</sup>F. W. Patten and F. J. Keller, Phys. Rev. **187**, 1120 (1969).

<sup>14</sup>In a recent attempt to test the Pooley-Hersh mechanism of color-center formation by F. J. Keller and F. W. Patten [(Solid State Commun. **7**, 1603 (1969)] it was concluded that recombination of an electron with a  $V_K$ -type center ( $\text{Cl}_2^-$  or  $\text{ClBr}^-$ ) may result in interstitial Cl atom formation. However, at the high temperatures we are working at, we observe only the decay of  $\text{Cl}_2^-$ , without a detectable increase in the concentration of the interstitial centers.

<sup>15</sup>The interstitial Cl ions  $\text{Cl}_i^-$  are not paramagnetic, and their behavior cannot be studied directly with EPR. The trapped  $\text{Cl}_i^-$ , called the  $I$  center, is unstable at 77 K in KCl, but there is evidence from the optical-

absorption measurements (Refs. 6 and 7) that a mobile interstitial halogen ion, just like a mobile interstitial halogen atom, may be trapped by  $\text{Na}^+$  or  $\text{Li}^+$  ions forming what one could call  $I_A(\text{Na}^+)$  or  $I_A(\text{Li}^+)$  centers. It seems reasonable to expect that  $\text{Cl}_i^-$  may also be stabilized up to an even higher temperature by pairs of  $\text{Na}^+$  or  $\text{Li}^+$  ions, producing  $I_{AA}$  and/or  $I_{A'A}$  centers.

<sup>16</sup>W. Hayes and J. W. Hodby, Proc. Roy. Soc. (London) **294A**, 359 (1966).

<sup>17</sup>D. Schoemaker, Bull. Am. Phys. Soc. **12**, 410 (1967).

<sup>18</sup>W. Hayes and G. M. Nichols, Phys. Rev. **117**, 993 (1960).

<sup>19</sup>C. J. Delbecq, D. Schoemaker, and P. H. Yuster, Phys. Rev. B **3**, 473 (1971).

<sup>20</sup>However, it is quite possible that such a center might be produced by x or  $\gamma$  irradiation at temperatures below 77 K.

<sup>21</sup>K. Bachmann and H. Peisl, J. Phys. Chem. Solids **31**, 1525 (1970).

<sup>22</sup>If the distribution of the  $\text{Li}^+$  or  $\text{Na}^+$  ions were random, and if the cross section for trapping interstitial Cl atoms were the same for both the nn and nnn pairs, then the  $H_{A'A}/H_{AA}$  concentration ratio should be exactly 2. The large difference in appearance and relaxation behavior of these centers does not allow one to determine this ratio accurately. One can only say that  $H_{AA}$  and  $H_{A'A}$  have comparable concentrations.

<sup>23</sup>H. M. McConnell, J. Chem. Phys. **25**, 709 (1956).

<sup>24</sup>G. E. Pake, *Paramagnetic Resonance* (Benjamin, New York, 1962).

<sup>25</sup>A recent paper in the field of motional effects in EPR which, apart from treating a simple case in detail, gives some representative references in this field is R. C. Hughes and Z. G. Soos, J. Chem. Phys. **52**, 6302 (1970).

<sup>26</sup>K. Bachmann and W. Känzig, Physik Kondensierten Materie **7**, 286 (1968).

<sup>27</sup>D. Schoemaker and E. L. Yasaitis, Bull. Am. Phys. Soc. **16**, 440 (1971).

## Resonant Phonon-Assisted Generation of Second-Harmonic Light

P. N. Keating and Ch. Deutsch\*

Bendix Research Laboratories, Southfield, Michigan 48075

(Received 25 November 1970)

The generation of second-harmonic optical radiation with the simultaneous absorption or stimulated emission of acoustical phonons is studied both theoretically and experimentally. A quantum theory of the processes involved is developed on the basis of perturbation theory. The analysis predicts that a multiple resonance in the output power should be observable as a function of the acoustical propagation angle for propagation close to normal to the fundamental optical beam. Experimental results are presented in which a double resonance peak is observed for 1.06- $\mu$  input optical radiation and 300-MHz longitudinal acoustical radiation in  $\text{LiNbO}_3$ . The observed angular separation between the two peaks agrees well with that expected for phonon-absorption and -emission contributions from a pole in the scattering amplitude at twice the fundamental optical frequency.

### I. INTRODUCTION

The generation of optical harmonics by mixing

intense light beams in optically nonlinear crystals has become a relatively common technique since the original classic work of Franken *et al.*<sup>1</sup> One